Ocean and Coastal Management 244 (2023) 106802

Contents lists available at ScienceDirect

Ocean and Coastal Management

journal homepage: www.elsevier.com/locate/ocecoaman

Spatiotemporal changes of coastal land use land cover and its drivers in Shanghai, China between 1989 and 2015

Chen Meng [a,1], Caiyan Wu [b,c,1], Jiong Wu [b], Qi Zhang [d], Liang Xin [e,f], Junxiang Li [b,*], Dezhi Li [a,**], Conghe Song [d]

[a] School of Ecological and Environmental Sciences, East China Normal University, Shanghai, 200241, China
[b] Department of Landscape Architecture, School of Design, Shanghai Jiao Tong University, Shanghai, 200240, China
[c] Department of Geography, Humboldt-Universität zu Berlin, 12489, Berlin, Germany
[d] Department of Geography, University of North Carolina at Chapel Hill, Chapel Hill, NC, 27599, USA
[e] Shanghai Municipal Institute of Surveying and Mapping, Shanghai, 200063, China
[f] College of Surveying and Geo-Informatics, Tongji University, Shanghai, 200092, China

ARTICLE INFO

Keywords:
Coastal zone
Socioeconomic factors
Urbanization
Spatiotemporal pattern
Gradient analysis
Partial least square regression
Canonical correlation analysis

ABSTRACT

The coastal zone, an ecotone that provides vital diverse ecosystem services, is one of the most ecologically fragile and sensitive areas on the Earth. It has been strongly influenced by human activities and climate change. Thus, understanding the spatiotemporal changes of land use land cover in the coast is an essential prerequisite for the comprehensive evaluation of coastal ecosystems and the promotion of sustainable development. This study investigated the spatial and temporal changes of land use land cover in the coastal zone of mainland Shanghai by using high spatial resolution aerial images, and the associated driving factors obtained from statistical yearbooks between 1989 and 2015. Our results show that the total land area in the coastal zone exhibited an increasing trend at an annual rate of 7.6% on average. The coastal urban land use also experienced substantial increases, with the degree of urban expansion reaching 42.1% in 2015. The coastal urbanization was at the cost of natural and semi-natural lands. Nearly 64.4% of agricultural land, 24.4% of ocean area within the buffer, 84.9% of fresh water, and 92.8% of the tidal flat had been converted to urban land during 1989–2015. The gradient analysis of land use land cover change along the north-to-south coastal line revealed the spatiotemporal patterns of total land, urbanization degree, and natural and semi-natural lands. The majority of the socioeconomic factors influenced land use land cover change in the coastal zone, positively contributing to the increase of public facilities' use of land, but negatively affecting the freshwater areas. These findings can provide insights for decision-making in the future for coastal land use land cover planning and management in Shanghai.

1. Introduction

The Coastal zone, an interface between land and ocean, provides favorable habitats for a wide variety of creatures and supplies vital goods and diverse ecosystems services to human beings, such as coastal hazard protection, and carbon sequestration (Arkema et al., 2015; Barbier et al., 2011; Chmura et al., 2003; Liu et al., 2021). The coastal zone is susceptible to the dual impacts of human activities and natural processes (Cazenave and Cozannet, 2014; Crain et al., 2009; Zhai et al., 2020; Ziaul Hoque et al., 2022; Zong et al., 2022), thus is ecologically fragile and sensitive to disturbance (de Andrés et al., 2023; Sannigrahi et al., 2019). For centuries, with the increase of urban population and expansion of urban areas, coastal reclamation and coastal land use changes have caused significant degradation of coastal ecosystems. It was estimated that, as of 2000, the low-elevation coastal zone covers only 2% of the world land area but supports 10% of the world's population (~600 million) and 13% of the world's urban population (~360 million) (McGranahan et al., 2007). With the increase of the world population and the associated rapid urbanization in the past two decades, it was projected that land use land cover change in the coastal

* Corresponding author.
** Corresponding author.
E-mail addresses: junxiangli@sjtu.edu.cn (J. Li), dzli@des.ecnu.edu.cn (D. Li).
[1] Co-first author.mengchen@stu.ecnu.edu.cn, caiyanwu@sjtu.edu.cn

https://doi.org/10.1016/j.ocecoaman.2023.106802
Received 12 May 2023; Received in revised form 9 July 2023; Accepted 8 August 2023
0964-5691/

zones will continue to increase, further aggravating landscape fragmentation (Liu et al., 2020b; Lu et al., 2022). Continued wetland reclamation will exacerbate conflicts of land resource supply and demands (Irwin and Bockstael, 2007; Marraccini et al., 2015; Zong et al., 2022). Understanding land use and land cover change is fundamental for land use dynamics research and the associated ecological consequences (Turner, 2005). Therefore, accurately mapping coastal land use land cover change and identifying the underlying drivers are essential to decision-making to support the sustainable management and conservation of coastal ecosystems (Olaniyi et al., 2012; Wang et al., 2022).

Worldwide, the increasing trend of urbanization in cities, especially coastal cities, accelerates the coastal land use land cover changes. The various goods and services provided by coastal ecosystems led to their over-exploitation for human usage, especially the demand for land for economic development (Olaniyi et al., 2012). It was projected that global urban land cover will increase by 1.2 million km^2 by 2030, nearly tripling the global urban land cover circa 2000, if the current trends of population growth continue (Seto et al., 2012). Rapid urban growth and population increase have resulted in huge land demand and coastal land transformation and reclamation. For example, nearly 50% of the salt marshes in New England vanished during the mid-1970s, and 35% of the world's mangrove forests disappeared in the 1980s owing to human activities and environmental pressures (Valiela et al., 2009). Meanwhile, China lost 58% (nearly 80,100 km^2) of its total coastal wetland between 1950 and 2014, which was mainly due to reclamation and infrastructure development (Sun et al., 2015). The reclaimed coastal wetland was usually transformed into multiple land use types, such as agriculture and industry in the cities (e.g., New York and New Orleans) (Temmerman et al., 2013), fishery (Wang et al., 2014), roads, ports, and other built facilities (Tian et al., 2016) in Chinese cities. With the transformation of coastal land use and land cover, issues, such as coastal erosion and species invasion, have been increasingly frequent since the 1990s, influencing the coastal ecosystem structure and functions (Cazenave and Cozannet, 2014; Chen et al., 2004; Kankam et al., 2022; Liu et al., 2020a, 2020b, 2021; Luan et al., 2016; Tan et al., 2022; Xin et al., 2023). Land reclamation caused serious impacts on coastal ecosystems and their services, such as the significant coastal landscape fragmentation and loss of biodiversity, destruction of habitats for fish and shorebirds, decline of bird species and fishery resources, reduced water purification ability, and even disappearance of gulfs and bays (Wang et al., 2014; Wu et al., 2018). Previous studies on land use land cover change primarily focused on the regional, national, and global scales without explicit emphasis on the coastal zone (Liu et al., 2020a; Tiando et al., 2021; Yim et al., 2018; Zhang et al., 2020a; Zhu et al., 2022; Ziaul Hoque et al., 2022). While the coastal land use land cover planning and management, especially coastal wetland conservation, must be integrated into local economic development plans (Yang et al., 2017). Time-series satellite images (e.g., Landsat) have long been considered as data sources for coastal research; however, they do not satisfy the fine-scale land use land cover change monitoring (Zhu et al., 2021), particularly for wetland. The utilization of high spatial resolution images can provide high-accuracy mapping of land use land cover information, and thereby can be used to examine the complex variations of coastal land use land cover change, and capture their subtle features of spatial details (Pan et al., 2023). Therefore, accurately identifying various types of coastal land use land cover types and monitoring their spatial and temporal pattens in the coastal zones are critical for both economic development and environmental conservation.

The land use land cover changes can be driven by diverse forces, including natural, socioeconomic, technological, political, and cultural factors (Brandt et al., 1999; Mitsuda and Ito, 2011). These driving forces can influence the coastal land use land cover change individually or collectively, and profoundly shape the structure and functions of coastal landscapes and ecosystems. For example, the reclaimed coastal wetlands between 1985 and 2010 in China reached nearly 754,697 ha. The reclamation was mainly driven by economic activities, often measured by Gross Domestic Production (GDP), and human population in the coastal region (Tian et al., 2016). The coastal aquaculture expansion in Southeast Asia was driven by natural factors (e.g., the presence of mangroves) and socioeconomic factors (e.g., institutional policies, capital investment, and market demand), and even the complex combinations of these factors (Akber et al., 2020). In a study conducted in Malaysia, population and its demographic variables, GDP, road density, river density, distance to road and river, etc. were selected as drivers to analyze the coastal land use changes (Olaniyi et al., 2012). In another study in Jiangsu, China, ten socioeconomic driving factors, such as urbanization rate and urban per capita housing area, were selected to study the coastal land use land cover change (Chuai et al., 2019). For coastal landscapes, the major drivers of land use and land cover change were concentrated in the socioeconomic domain, reflecting the impacts of human activities (Martins et al., 2012). Therefore, quantifying the complex impacts of socioeconomic driving factors on coastal land use land cover changes and their contributions is of great importance. The quantification can provide critical data for the comprehensive management and coordination of different land use land cover types and socioeconomic activities.

Shanghai is one of the most urbanized cities in China. It has developed rapidly in the past three decades with an average increase of 13.5% in annual GDP (SBS, 2019), making it known as the engine of economic development in the Yangtze River Delta. In Shanghai, rapid urbanization has caused drastic land use and land cover change (Li et al., 2013). However, how urbanization impacts coastal land use land cover change has yet to be fully assessed. Located at the frontier of the Yangtze River Delta and bordering the East China Sea, Shanghai has a long shoreline and rich coastal wetland resources. Therefore, it is an ideal place to investigate the impacts of urbanization on coastal land use land cover change. This study aims to address the following questions: (1) How does the coastal land use and land cover change over time? (2) What are the spatial and temporal patterns of land use land cover change along the coastal zone? (3) How are the socioeconomic factors associated with the land use and land cover change in the past three decades? Answers to these questions will provide insights for decision-making in coastal wetlands conservation and restoration, and sustainable management in Shanghai and other coastal zones in other parts of the world in similar settings.

2. Materials and methods

2.1. Study area

Shanghai lies in 30°40′-31°51′N and 120°52′-122°21′E, and locates at the estuary of the Yangtze River and borders the East China Sea to the east, the Hangzhou Bay to the south and Jiangsu and Zhejiang Provinces in the west. It is bounded by 460 km shoreline, of which the mainland coastline is 173 km. The mainland part of the coastline starts from the estuary of Liuhe in Taicang county of Jiangsu province in the north, and ends at the Jinsiniang Bridge on the northern shoreline of Hangzhou Bay in the south. The remaining shoreline is mainly those around the three islands of Chongming, Changxing, and Hengsha (Shi et al., 2003). In the past decades, the land use land cover composition and its landscape patterns in the coastal area of Shanghai have experienced dramatic changes due to the development of the Waigaoqiao Harbor District, the Pudong International Airport, the Yangshan International Deepwater Port, the Chemical Industrial Park, and the New City of Lingang, etc. (Huang et al., 2016; Xin et al., 2023; Zhang et al., 2020b). During the rapid urbanization from these developments, losses of natural and semi-natural lands and the associated habitat fragmentation have been widely observed (Xin et al., 2023). In addition, the sedimentation and reclamation further altered the coastal landscape and the coastline in the coastal zone in Shanghai. For example, the potential tidal flat area within −5 to 0 m above sea level in Shanghai reached 3000 km^2 in the year 2000; there were a total of 873 km^2 of tidal flat that has been reclaimed from 1949 to 2001, and 70% of the reclamation occurred after 1987. The reclaimed land areas were mainly used for aquaculture and agriculture, industry, tourism, and green spaces (Su, 2003). Given the continuous changes in the coastline and the reclamation of the tidal flat areas in the past decades, our study area was set within a buffer area along the 173 km long mainland coastline, whose inner boundary is 5 km inward from the coastline of 1989, while the external boundary is 5 km outward from the coastline of 2015 (Fig. 1). The coastal areas in the three islands of Chongming, Changxing, and Hengsha were not included.

2.2. Data collection and processing

This study uses high spatial resolution aerial photos from 1989 to 2015 to derive time series land use land cover data. Markov transition matrix and the gradient analysis were then utilized to quantify the spatial and temporal changes of land use land cover in the coastal zone. Socioeconomic data, partial least square regression (PLSR) and the canonical correlation analysis (CCA) were employed to identify the drivers of land use land cover changes. The flowchart below showed the main steps of data analysis in this study (Fig. 2). The details were presented in the following sections.

2.2.1. Land use land cover classification and digitization

In this study, time series color-infrared and true-color aerial photos, which were acquired by airborne sensors and provided by the Shanghai Municipal Institute of Surveying and Mapping, were utilized to derive land use land cover types. The color-infrared photos with a spatial resolution of 2.5 m were acquired in 1989, 1994, 2000, and 2005. True-color photos with a spatial resolution of 1 m were acquired in 2010 and 2015. We adopted the land use land cover classification scheme from Li et al. (2013), of which the category of water was further divided into fresh surface water, sea water, and tidal flat to accommodate the complex land cover composition in the coastal zone. Therefore, we designed a 10-class land use land cover scheme, including residential, public facility, industrial, traffic, agricultural, green land, fresh water, sea water, tidal flat, and others (such as under-construction sites). Here, fresh water denotes the surface water bodies of lakes, ponds, rivers, etc., while sea water denotes the offshore sea water within the buffer zone. We further reclassified these ten classes into two major groups, urbanized land (i.e., residential, industrial, public facilities, traffic land) and natural & semi-natural land (i.e., green land, fresh water, sea water, tidal flat, and agricultural land). The time series land use land cover types were mapped using the approach of backdating and object-based integration proposed by Yu et al. (2016). First, each land use land cover type was visually interpreted and digitized from the true-color photos of 2015 in the platform ArcGIS (version 10.5, ESRI). Then, ground truthing was performed using 1000 randomly selected samples for all types except sea water to validate the classification, which showed that the overall accuracy was over 90%. Third, we used the land use land cover map of 2015 as referenced and overlapped on the historical photos to interpret and map the land use land cover of each year of 2010, 2005, 2000, 1994, and 1989, separately. The final maps of historical land use land cover were shown in Fig. 3 and in the supplementary Fig. A.1. The overall classification accuracies for 1989, 1994, 2000, 2005, 2010, and 2015 were 93.9%, 95.3%, 95.8%, 96.3%, 94.95%, and 91.63%, respectively.

2.2.2. Land use and land cover change detection

The Markov chain was employed to quantitatively model the spatial and temporal patterns of land use and land cover change in the five time periods of 1989–1994, 1994–2000, 2000–2005, 2005–2010, and 2010–2015. The Markov model is useful to track past land use and land cover changes and project future landscape dynamics (Urban and Wallin, 2002), and has been widely used to study terrestrial and coastal land use and land cover change (Bracchetti et al., 2012; Eddy and Gergel, 2015; Ekumah et al., 2020; Kayhko et al., 2011; Pontius et al., 2004). Markov process is a random process that describes a system that changes from one state to another during each period. It assumes that the probability distribution over the next state is determined by the current state (Guan et al., 2011; Zhu et al., 2021). The fundamental component of the Markov model is the transition matrix that characterizes the changes between different land use land cover types over multiple time periods. In this study, a transition matrix was used to quantify both the stable land use land cover types and the probability of one land use land cover type changing to another in each period. Given that the number of land use and land cover types was 10, a 10 × 10 empirical transition matrix was generated for each of the five time periods using the Tabulate area tool in ArcGIS to get the area and probability of each land use land cover type. The transition matrix model is as follows.

$$S_{ij} = \begin{bmatrix} S_{11} & S_{12} & \dots & S_{1n} \\ S_{21} & S_{22} & \dots & S_{2n} \\ \dots & \dots & \dots & \dots \\ S_{n1} & S_{n2} & \dots & S_{nn} \end{bmatrix} \tag{1}$$

where S_{ij} is the area of conversion from category i to category j of land use and land cover types from the initial to the final phase, and n was the total number of types in land use.

2.2.3. Spatial and temporal dynamics of land use land cover along the coastal line

To further explore the spatial and temporal changes in land use land cover along the coastal line of mainland Shanghai, a latitudinal gradient was set up with grids of 10 km along the coastal line from the north to

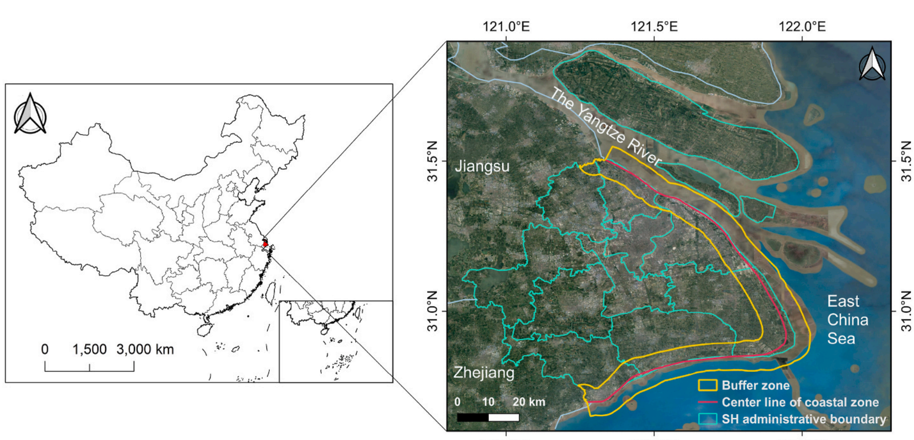

Fig. 1. Study area along the coastal line on the mainland of Shanghai.

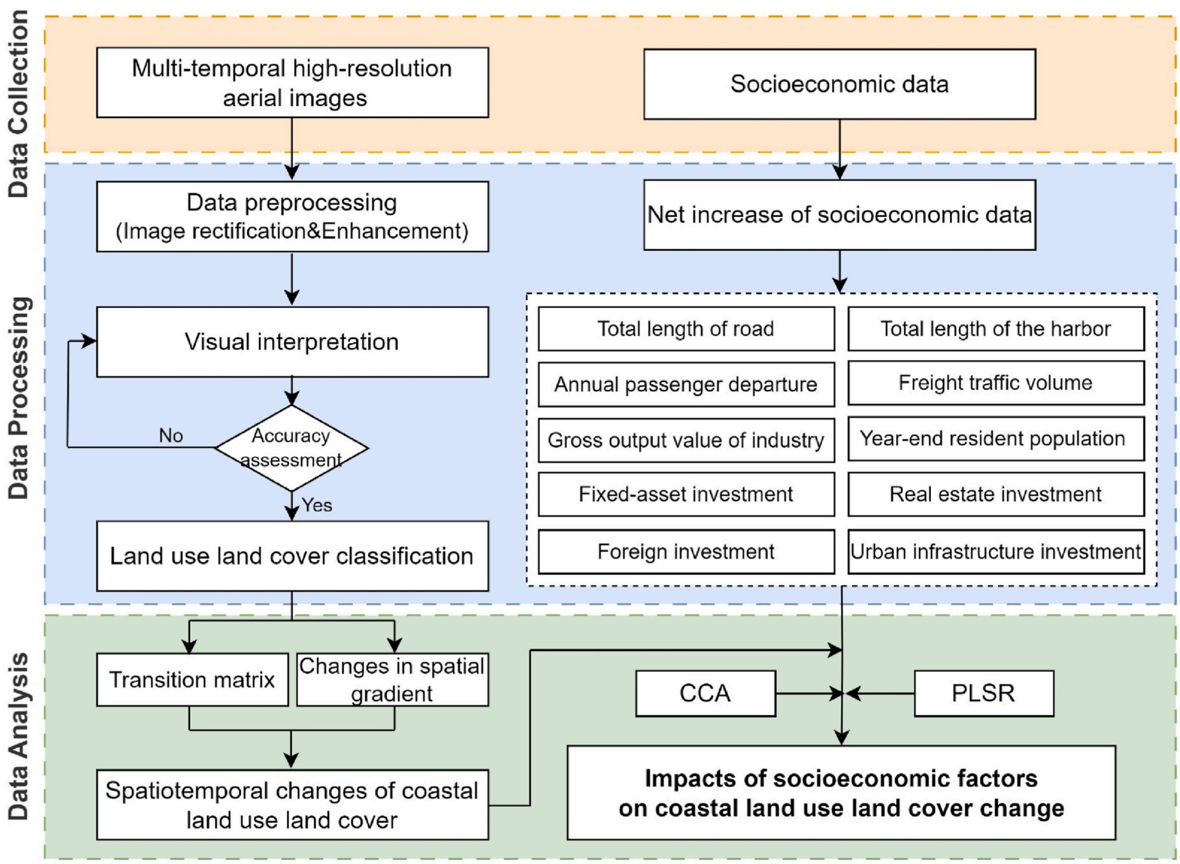

Fig. 2. Flowchart of data analysis in this study.

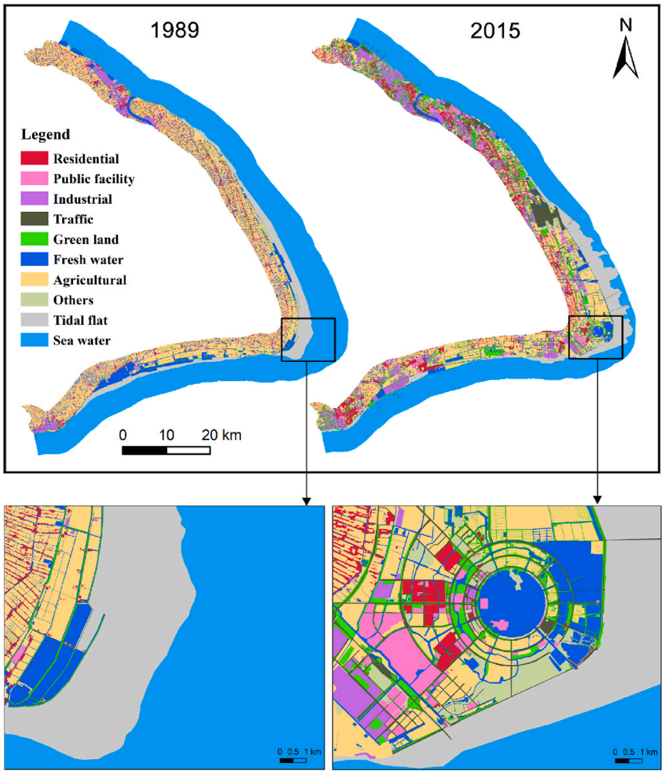

Fig. 3. The maps of land use land cover in the mainland coastal zone of Shanghai in 1989 and 2015 (The sub-plots show the Dishui Lake area).

the south. We finally got 18 grids (shown in Fig. 7-a). The area of each grid is shown in Table 1.

Table 1
The land area of each grid from north to south along the coastal line (km^2).

Grid No.	Land area	Grid No.	Land area
1	26.6	10	141.2
2	108.4	11	145.6
3	104.2	12	112.5
4	104.3	13	100.3
5	108.0	14	101.3
6	109.5	15	107.6
7	111.3	16	116.7
8	126.1	17	102.0
9	128.6	18	44.8

2.2.4. Selection of socioeconomic driving factors

According to previous studies (Chuai et al., 2019; Olaniyi et al., 2012), ten socioeconomic variables, including the total length of road (X_1), the total length of the harbor (X_2), annual passenger departure (X_3), freight traffic volume (X4), gross output value of industry (X_5), year-end resident population (X_6), fixed-asset investment (X_7), real estate investment (X_8), foreign direct investment (X_9), and urban infrastructure investment (X_{10}), were selected as the driving factors to examine the impacts of urbanization on coastal land use land cover dynamics in Shanghai. All the data of these variables were collected from the yearly statistic book of Shanghai. We used the averaged net increase area of nine land use land cover types, (i.e., residential, public facility, industrial, traffic, agricultural, green land, fresh water, tidal flat, and others) and a net increase of ten socioeconomic factors over each subperiod (i.e., the period of 1989–1994, 1994–2000, 2000–2005, 2005–2010, 2010–2015) to assess the potential impacts of socioeconomic factors on coastal land use land cover change of Shanghai.

2.3. Statistical analysis

2.3.1. Regression analysis

To identify the impacts of socioeconomic factors on land use land cover types, we quantified their relationship using linear regression analysis. Furthermore, the significant socioeconomic factors for each land use land cover type were selected as independent variables in the partial least square regression (PLSR) model.

The PLSR analysis is a robust multivariate regression method that is specifically useful when the predictors exhibit collinearity (Shi et al., 2013; Wold et al., 2001). It has been widely used to explore the drivers of urban growth (Li et al., 2018), agriculture ecosystem services (Yu et al., 2018). PLSR uses the variable importance in projection (VIP) score to evaluate the relative importance and the contribution of each variable to the dependent variable (Li et al., 2014). A value of Variable Importance in the Projection (VIP) greater than 1 indicates that the predictor variable is significantly important to the dependent variable (Wold et al., 2001). In this study, the regression coefficients were used to quantify the direction of the impact of each variable, and the variable importance of socioeconomic factors was identified using VIP scores. The relationship between the dependent and independent variables in the PLSR model was defined as the following:

$$y = a + a_1X_1 + a_2X_2 + \ldots + a_nX_n \quad (2)$$

where y is the average net increase of land use land cover area for each period, X_i is the averaged net increase of socioeconomic factor i, a_i is the regression coefficient of variable X_i, where $i = 1, .., n$.

The data of all dependent and independent variables were transformed using z-score normalization before PLSR analysis.

$$Z=(x-\mu)/SD \quad (3)$$

where x is the observed value; μ is the mean value; SD is the standard deviation.

2.3.2. Canonical correlation analysis

We further estimated the correlation between socioeconomic factors and the area of land use land cover types using canonical correlation analysis (CCA). The CCA is an approach for estimating the correlation between two sets of variables including possibly more than one variable in each set (Grimm and Yarnold, 2000), and thus one of the standard tools for multivariate analysis. Different from the principal component analysis that seeks the maximum variance in one data set, CCA carries the goal of maximizing the association between two latent variables constructed from the two data sets, respectively (Härdle and Simar, 2019). The specific steps of CCA analysis were shown as follows:

First, we chose two sets of variables. The first set of variables were the two socioeconomic factors X= (X_1, X_2), and the second was the areas of two kinds of land use land cover types Y= (Y_1, Y_2). Here we mainly analyzed highly related land use land cover types for the combines, of which Y_2 was one of the top three types that converted from Y_1 to Y_2 based on the Markov model.

Next, we created the linear combination of the two sets of variables using the following equations (Zhou et al., 2021):

$$\begin{cases} u = L_1X_1 + L_2X_2 \\ v = M_1Y_1 + M_2Y_2 \end{cases} \quad (4)$$

where u and v are the canonical variables, L and M are the coefficients of the linear combination, X_i and Y_i are the averaged net increase of the area of land use land cover and socioeconomic factors for each period, and the correlation coefficient is λ. We finally obtained the correlation coefficient between the two canonical variable pairs in this study.

$$\lambda = \frac{COV(u,v)}{\sqrt{var(u)} \bullet \sqrt{var(v)}} = \frac{COV(LX,MY)}{\sqrt{var(LX)} \bullet \sqrt{var(MY)}} \quad (5)$$

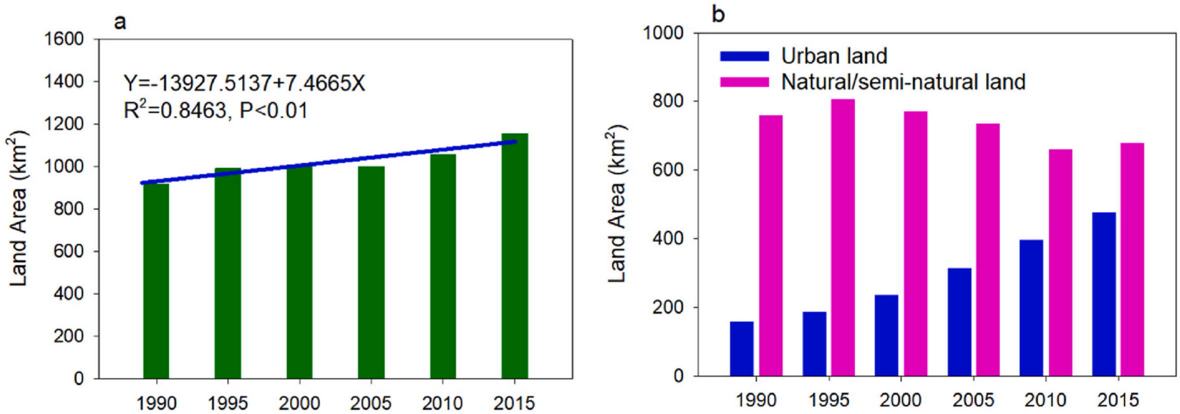

Fig. 4. Land use land cover changes in the coastal zone in Shanghai from 1989 to 2015.

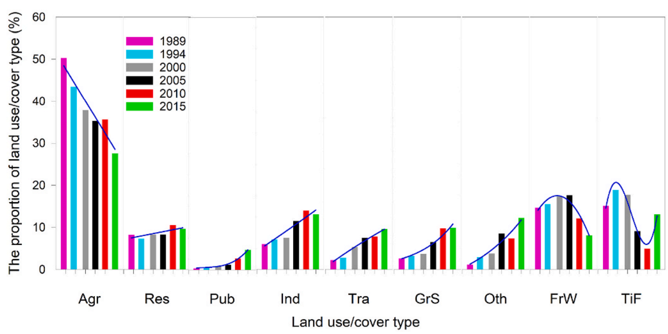

Fig. 5. The variations and fitting curves of land use land cover type proportion in the coastal zone from 1989 to 2015. Agr-Agricultural land; Res-residential land; Pub-Public facilities; Ind-Industrial land; Tra-Traffic land; GrS-Green Space; Oth-Other land; FrW-Fresh water; TiF-Tidal flat.

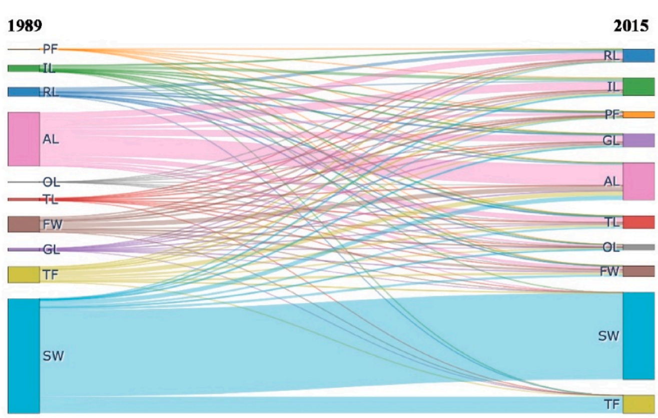

Fig. 6. The Sankey diagram shows the transformation between land use land cover types from 1989 to 2015 in the coastal zone of Shanghai. RL: Residential land; PF: Public facilities; IL: Industrial land; TL: Traffic land; GL: Green land; FW: Fresh water; AL: Agricultural land; OL: Other land (others); TF: Tidal flat; SW: Sea water.

3. Results

3.1. Land use land cover change in the coastal zone

The total land area, excluding sea water, in the coastal zone increased from 918.23 km^2 in 1989 to 1156.17 km^2 in 2015, by nearly 1.26 times, exhibiting a generally increasing trend over time (Fig. 4-a). The average annual rate of the increase was 7.61%. The urbanized land monotonically increased from 158.80 km^2 in 1989 to 476.39 km^2 in 2015, while the share of the urban land use land cover in the total land area increased from 17.29% in 1989 to 41.20% in 2015. The compound annual growth rate reached 4.32%. Meanwhile, the total natural and semi-natural land (excluding sea water) decreased from 759.43 km^2 in 1989 to 679.78 km^2 in 2015, a total decline of 79.65 km^2, albeit with fluctuation (Fig. 4-b).

The variations of the proportion of each land use land cover type (excluding sea water) are shown in Fig. 5. All the urban land use land cover types increased rapidly from 1989 to 2015. Residential area, industrial area, and traffic land exhibited overall increase trends, from 8.26%, 6.06%, and 2.27% in 1989 to 9.67%, 13.14%, and 9.59% in 2015, respectively. Public facilities and other land presented exponential increase trends, from 0.32% to 0.39% in 1989 up to 4.71% and 4.09% in 2015, respectively. Natural and semi-natural land generally showed a decreasing trend between 1989 and 2015. Agricultural land exhibited a sharp decrease from 50.30% to 27.59%. Fresh water presented a quadric change pattern, firstly increasing from 14.69% to the peak of 17.64% and then decreasing to 8.14%. The tidal flat displayed a cubic polynomial change trajectory and decreased from 15.13% in 1989 to 13.06% in 2015. Only green space kept an exponentially increasing trend, from 2.60% to 9.91%.

The land use land cover types in the coastal zone experienced a dramatic change from 1989 to 2015. Here we only showed the transitions and changes between the full study period of 1989–2015 (Fig. 6); for the transition and change of land use land cover in each subperiod, please see the supplementary Fig. A.2. Nearly all the urbanized land categories exhibited substantial changes in each period; approximately 20%–50% of the natural and semi-natural land have been converted to urban land use in each period; large reclamation occurred in the periods of 1989–1994, 2005–2010, and 2010–2015 (Fig. A.2). In the entire study period, large amounts of natural and semi-natural lands were transformed to urbanized land (Fig. 6), among which 206.64 km^2 (64.4%) of the agricultural land were transformed to industrial land (67.69 km^2), residential land (54.31 km^2), traffic land (43.76 km^2), public facilities (23.41 km^2), and other land (15.46 km^2). There were 239.16 km2 (24.4%) of ocean area transformed and mainly converted to tidal flat (141.85 km^2), agricultural land (37.42 km^2), fresh water (19.20 km^2), and traffic land (16.93 km^2). About 128.82 km2 of the tidal flat (92.75%) was lost during 1989–2015, due to transformations mainly to agriculture (38.17 km^2), traffic land (18.22 km^2), fresh water (17.50 km^2), industrial land (17.17 km^2), other land (12.23 km^2), and green land (12.00 km^2). Meanwhile, 114.44 km^2 of the fresh water (84.9%) was converted to agricultural land (44.55 km^2), industrial land (17.69 km^2), green land (15.14 km^2), residential land (14.58 km^2), traffic land (11.99 km^2), and public facilities (8.95 km^2), respectively.

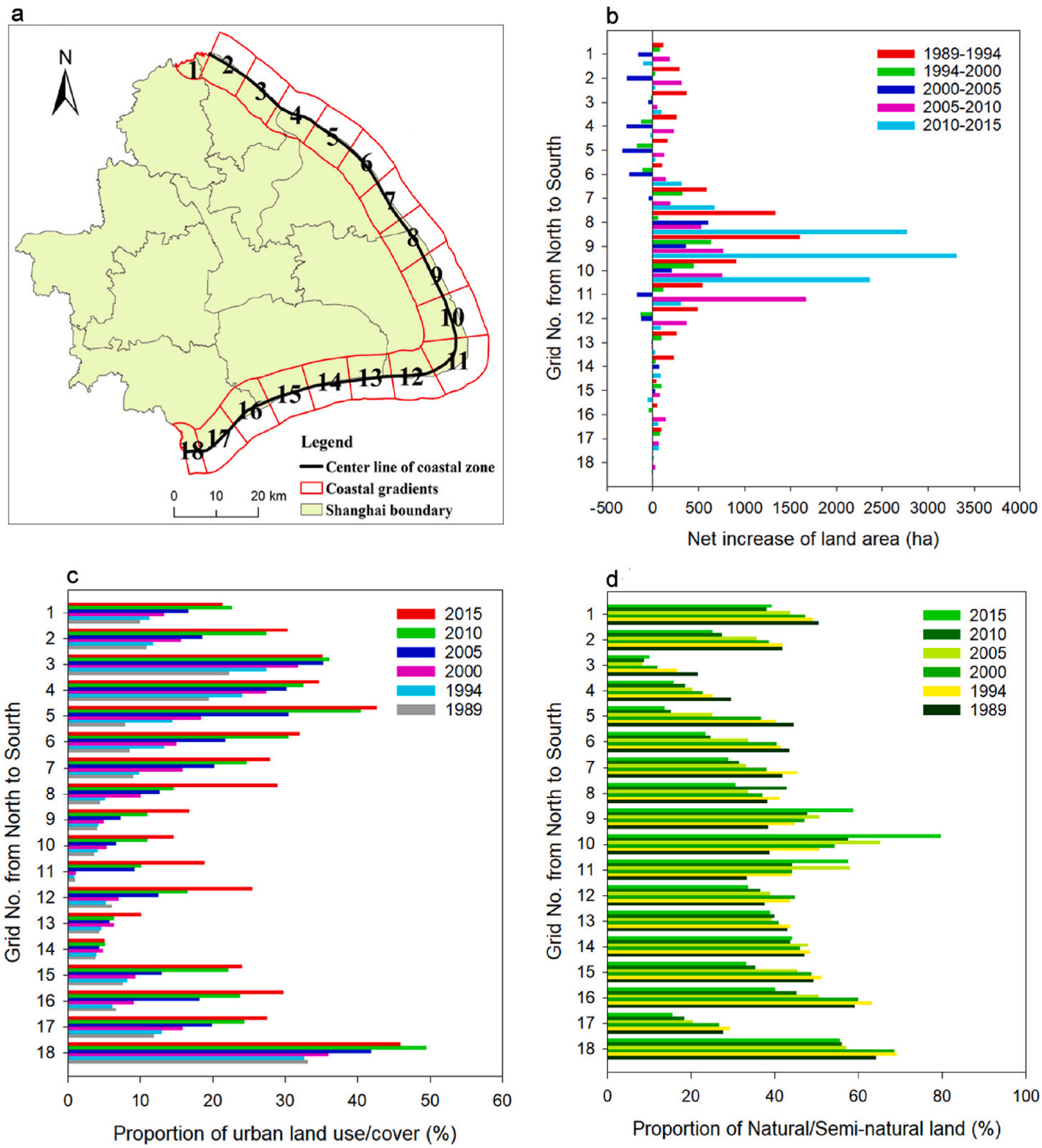

Fig. 7. The defined girds and the area changes in the grids from 1989 to 2015.

Table 2
PLSR model for public facility and fresh water and its driving factors.

Equations of PLSR Models	R^2
$Y_{public\ facilty'} = 0.9477 + 0.1949*X_3'+0.1822*X_4'+0.1952*X_5'+0.1913*X_8'+0.1955*X_9'$	0.905
$Y_{fresh\ water'} = -0.2876-0.2309*X_4'-0.2320*X_5'-0.1239*X_6'-0.2314*X_7'-0.2476*X_{10}'$	0.937

Note: $X_3'\sim X_{10}'$ are the scaled variables of $X_3\sim X_{10}$ using z-score normalization, X_3: annual passenger departure, X_4: freight traffic volume, X_5: gross output value of industry, X_6: year-end resident population, X_7: fixed-asset investment, X_8: real estate investment, X_9: foreign direct investment, X_{10}: urban infrastructure investment. $Y_{public\ facility'}$, and $Y_{fresh\ water'}$ are the scaled variables of public facility and fresh water using z-score normalization, respectively.

3.2. Spatiotemporal patterns of land use land cover change in the coastal zone

There were 18 grids along the coastal line in Shanghai (Fig. 7-a). Each grid had a net increase in land area except for the 5th grid, but the land area in each grid varied greatly from north to south between 1989 and 2015. Nearly all grids had a net increase in land area during the periods of 1989–1994 and 2005–2010, while in the other periods, the increase in land area mainly occurred in the 7th to 11th grids where large amounts of reclamation happened. Only a few net decreases were observed in the 4th, 5th, and 6th grids during the periods of 1994–2000 and 2000–2005 (Fig. 7-b). From the first grid in the north (the 1st) to the last one in the south (the 18th), there was a net increase in the proportion of urban land use land cover type, each grid exhibited a sharp increasing trend in the proportion of urban land use land cover type over time except for the 14th grid (Fig. 7-c). From 1989 to 2015, the least

Table 3
VIP value of the PLSR models for public facility and fresh water.

Land use land cover type	X_3	X_4	X_5	X_6	X_7	X_8	X_9	X_{10}
Public facility	1.016	0.949	1.017	–	–	0.997	1.019	–
Fresh water	–	1.060	1.065	0.569	1.062	–	–	1.136

Note: X_3: annual Passenger departure, X_4: freight traffic volume, X_5: gross output value of the industry, X_6: year-end resident population, X_7: fixed-asset investment, X_8: real estate investment, X_9: foreign direct investment, X_{10}: urban infrastructure investment.

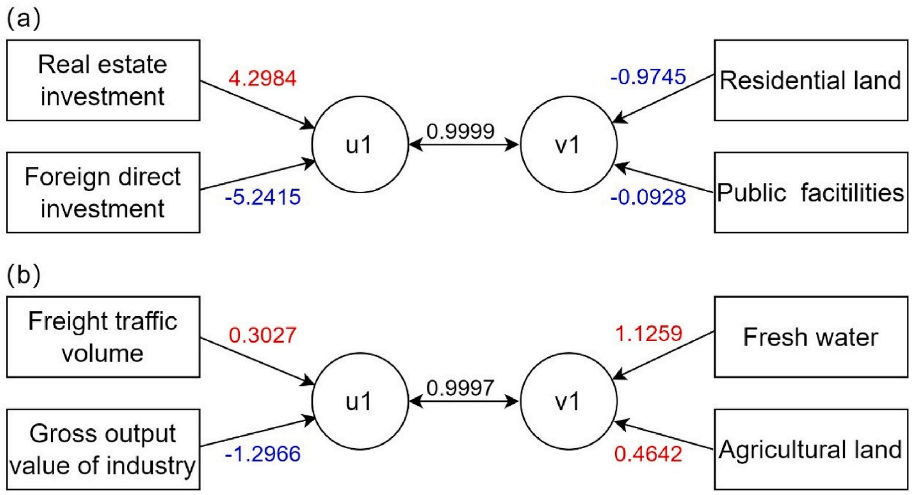

Fig. 8. Canonical correlation analysis of socioeconomic factors and land use land cover types.

increase in urban land use land cover proportion was 1.39 times, which occurred in the 18th grid, while the largest is nearly 20 times which occurred in the 11th grid. The proportion of natural and semi-natural land showed three patterns of variation. The first exhibited continuous decrease trends in the northern coastal zone from grid 1st to 7th and in the southern grids of 13th, 15th, and 17th. The second exhibited increased trends over time in the 9th, 10th, and 11th grids. The third presented a first increase and then decrease trend (Fig. 7-d).

3.3. Driving forces of land use land cover change in the coastal zone

The results of linear analysis and PLSR models built for different land use land cover types showed that the partial socioeconomic factors influenced the coastal land use land cover change in Shanghai (supplementary Table A.1 and Table 2). Most of the socioeconomic factors positively related to the land area of public facilities, suggesting that the selected socioeconomic factors, such as annual Passenger departure (X_3), freight traffic volume (X_4), and real estate investment (X_8), tend to facilitate the increase of urban land use types. For natural and semi-natural land use types, the majority of the socioeconomic factors negatively related to the area of freshwater, including freight traffic volume (X_4), gross output value of industry (X_5), year-end resident population (X_6), fixed-asset investment (X_7), and urban infrastructure investment (X_{10}). The socioeconomic factors can explain contributions to the area variances of 90.5%, and 93.7% for the public facility and fresh water, respectively (Table 2).

The factors with their variable importance in the projection (VIP) values equal to or greater than one means that they have significant influences on land use changes. According to the VIP value of the socioeconomic factor to public facilities and fresh water (Table 3), we can rank the factor's contribution to coastal land use change in Shanghai. The main drivers for public facilities were ranked by foreign direct investment (X_9), the gross output value of industry (X_5), and annual Passenger departure (X_3) in sequence according to their VIP value. While fresh water was mainly influenced by urban infrastructure investment (X_{10}), the gross output value of industry (X_5), fixed-asset investment (X_7), and freight traffic volume (X_4) in sequence.

Canonical correlation analysis (CCA) between socioeconomic factors and different land use land cover types was shown in supplementary Table A.2, which revealed that most of socioeconomic factors had impacts on land use land cover change. For the urban land type, we are interested in how real estate and foreign investment correlate and can both influence urban land change through the development of residential areas and public facilities. Through CCA (Fig. 8), the two constructed latent variables (i.e., υ1 & ν1) had a maximum correlation with a coefficient of 0.9999. Given the negative correlations between the land change (i.e., residential land and public facilities) and ν1 as well as the negative correlation between foreign investment and υ1, we found that foreign investment contributes to the growth of urban land expansion, particularly in areas for residential purposes and public facilities, while controlling for real estate. For natural & semi-natural land type, the CCA result showed that two constructed latent variables (i.e., υ1 & ν1) had a maximum correlation with a coefficient of 0.9997. The freight traffic volume can positively contribute to the fresh water and agricultural land change, while negative correlations existed between the gross output value of industry, and fresh water and agricultural land.

4. Discussion

4.1. Characteristics of Shanghai coastal land use land cover change

The coastal land in Shanghai experienced a rapid urbanization process in the past three decades. A large amount of natural and semi-natural land had been transformed into the urban land use type. The total area of urban land use land cover had grown exponentiallly and increased three times by the end of 2015 (Fig. 4-b), while each kind of urban land use type followed a steady or fast-growing trajectory from 1989 to 2015 (Fig. 5). The land urbanization rate, i.e., the proportion of the total urban land use types, reached 41.2%. The urbanized land increasing trend was similar to that in the entire coastal provinces in China where the urbanization also exhibited an exponentially growing trend, and the proportion of total urban land increased from 5.21% to

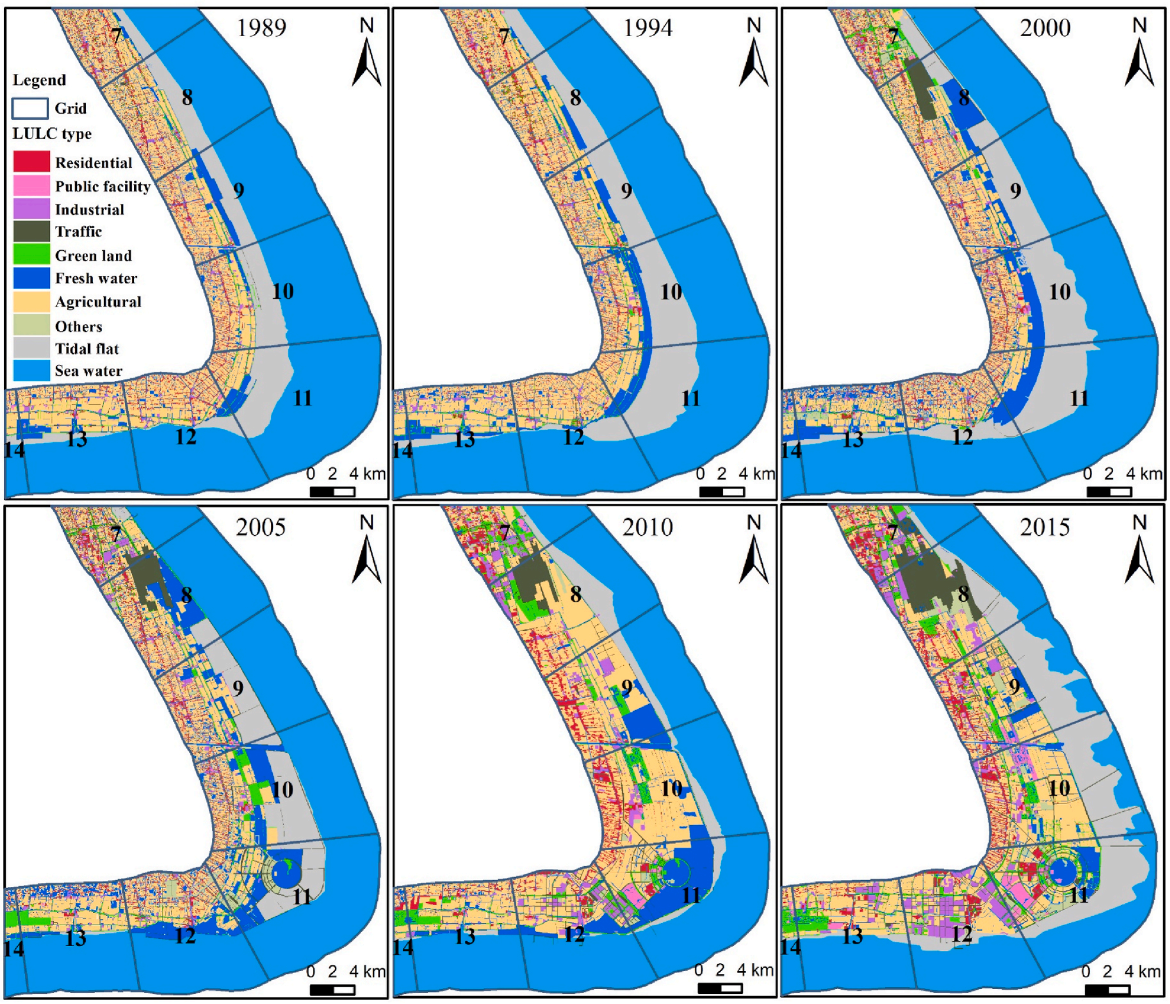

Fig. 9. The grids with drastic land use land cover changes and dynamics.

9.79% from 1985 to 2020 (Zhu et al., 2022). The trend was also similar to that in the 48 cities along the entire mainland coastal line where the urban land proportion increased from 7.73% to 11.59% from 1990 to 2015 (Zhang et al., 2020a). However, the land urbanization degree in Shanghai was far higher than those in other cities in the entire coastal areas of Chin In addition, our study showed that the coastal urbanization in Shanghai was at the cost of a large amount of natural and semi-natural land. Specifically, 64.4% of agricultural land, 62.5% of fresh water, and 37.8% of tidal flat have been converted to urban land use from 1985 to 2015, which were far larger than those in the entire coastal cities where 5.1% of agricultural land, 5.97% of water surface, 1.54% of grassland have been converted to urban land on average (Zhang et al., 2020a).

The land area in the coastal zone in Shanghai continuously increased and exhibited high spatiotemporal dynamics and drastic land use transitions in the past three decades. Firstly, the total coastal land area exhibited a generally increasing trend over time (Fig. 4-a) due to coastal reclamations to meet the great demand for land resources during rapid urbanization and industrialization in Shanghai. In the past decades, China's coastal areas experienced a dramatic urbanization process, which resulted in a vast demand for land resources (An et al., 2007; Cao and Wong, 2007; Sun et al., 2015). For instance, coastal reclamations have reduced more than 50% of coastal wetlands in China since 1949 (Wang et al., 2014). With such a background in China and the ambition of world city construction (Wu, 2000), Shanghai has undergone a rapid urbanization process and population increase (Wu et al., 2023), which brought in a large demand for land resources and stimulated coastal reclamation. As a result, 197.93 km^2 of the coastal wetland in the Pudong area of Shanghai were transformed between 1989 and 2013, and more than 80% of them were developed for agricultural, industrial, and urban land uses (Wu et al., 2018), while 580.39 km^2 of the coastal wetland in the entire coastal area in Shanghai has been reclaimed from 2002 to 2010 (Tian et al., 2016). Our results showed that 367.98 km^2 of coastal wetland around the mainland of Shanghai (including 128.82 km^2 of tidal flat and 239.16 km^2 of ocean area) had been reclaimed from 1989 to 2015.

Secondly, the coastal land use land cover types presented a very high spatial and temporal dynamic from 1989 to 2015. The longitudinal spatiotemporal analysis along the coastal line showed that high dynamics mainly occurred within two segments, grid 2–3 and grid 8–12, where large increases in land area were presented, and the large-scale increases happened in the periods of 1989–1994 and 2010–2015 (Fig. 7-b, Fig. 9). This was mainly due to a series of policies implemented by the central government in Shanghai, such as the industrial modernization since the 1980s, the Pudong New Area opening and development initiated in 1990, the ambitious planning to construct an international center for economy, finance, trade, and shipping, etc. Under such policy benefits, many large projects have been initiated and sequentially constructed along the coastal line, such as the Bao Steel company's I-III constructions from 1979 to 1998, the series constructions of Waigaoqiao Port Project I to VI during 1991–2010, the Pudong international airport from 1996 to 2015 (1996–1999, I stage, 2003–2008 II, and 2015–2019 III, 2021–2025, IV), the New city of Lingang development started in 2003, Shanghai Chemical Industrial Park started from 1996, etc. These projects largely promoted the construction of traffic roads and public facilities as well as residential areas, thus enhancing coastal urbanization. As a result, the urban land use land cover types exhibited dramatic increases in each grid (Fig. 7-c). Furthermore, a large amount of natural and semi-natural land, like tidal flat and agricultural land, had been transformed to urban land use in the corresponding grid except for the grid of 9, 10, and 11 where a lot of sea water and tidal flat had been enclosed and reclaimed (Fig. 7-d, Fig. 9). Therefore, longitudinal analysis is a robust method to demonstrate the spatial and temporal coastal land use land cover change over time.

In addition, due to the ecological city construction as one of the goals in the master planning of Shanghai, a series of forest parks and wetland parks have been constructed along the coastal line, such as the Paotaiwan Forest Park (2005–2007), the Shanghai Binjiang Forest Park (2004–2007), the Shanghai Binhai Forest park (2006 opened), the Shanghai Haiwan Forest park (1999–2006), which resulted in continuous increases of natural land in the past decades (Fig. 5).

Thirdly, the coastal land use land cover types experienced drastic transformation and exhibited high dynamics. Land use transition maps showed that the interconversion between different land use types in Shanghai coastal areas from 1989 to 2015 reflects the impacts of urbanization on land use land cover changes, characterized by high transformations between artificial land use types and natural and semi-natural land use types, as well as reclamation of tidal flat and sea water. The Dishui Lake (locates in grid 11) in the Lin-gang new city, now called the Lin-gang Special Area which is part of China's (Shanghai) pilot free trade zone, located at the Nanhui Cape in Pudong New Area has been completely constructed on the reclaimed land and can mostly exemplify the drastic land use land cover change happened in the coastal area in Shanghai. The constant shifting of land use and land cover reflects the diverse demand to satisfy the rapid urbanization of land resources in Shanghai.

4.2. Drivers of coastal land use land cover change

Coastal land use land cover changes were mainly driven by natural and socioeconomic factors, such as the natural geographic factors including DEM, vegetation, soil, precipitation (Olaniyi et al., 2012; Zong et al., 2022), the socioeconomic factors of economy, urbanization, GDP, population (Tian et al., 2016), and even the government policy reflected by the combination of geographic locational, technological, economic, institutional, and social factors (Akber et al., 2020). Our study only considered the socioeconomic factors but omitted the natural factors due to the fact that the coastal area in Shanghai lies on the edge of an alluvial plain with slight elevation variations. The partial least square regression analysis showed that there was a strong relationship between public facilities and the majority of the socioeconomic factors (Table 2), and socioeconomic development had enormously driven the urbanization in the coastal zone in Shanghai in the past three decades. Firstly, the policy support from national and municipal governments promoted the rapid urbanization of Shanghai. The 14th National Congress of the Communist Party of China in 1992 proposed a major strategic decision to build Shanghai as one of the international economic, financial, and trade centers, which initiated Shanghai's rapid urbanization. Response to this decision, Shanghai municipal government issued Urban Master Planning of Shanghai (1999–2020) which aimed primarily to construct Shanghai as an international center of economic, financial, trade, and shipping in 2020 and resulted in a dramatic urban growth with the huge land resources demand. Previous studies demonstrated that the urban area of Shanghai had tripled during 1985–2015, which was strongly driven by seven socioeconomic factors (Wu et al., 2023).

Secondly, the socioeconomic conditions had been greatly developed and substantially promoted urbanization in Shanghai. For example, the factors of the total length of road (X_1), total length of the harbor (X_2), annual passenger departure (X_3), freight traffic volume (X_4), the gross output value of industry (X_5), year-end resident population (X_6), fixed-asset investment (X_7), real estate investment (X_8), foreign direct investment (X_9), and urban infrastructure investment (X_{10}) increased 4.5, 7.9, 4.5, 3.3, 21.8, 1.8, 29.6, 183.2, 43.7, and 39.5 times, respectively from 1989 to 2015, which had together driven the urban land use growth and stimulated the urbanization in the coastal area. The coastal urbanization, in turn, resulted in a sharp decrease in natural and semi-natural land, although the Chinese government had issued a strict arable land protection policy which had set up a bottom line to arable land area to ensure the food supply (Li and Sun, 1997; Tian et al., 2016; Xie et al., 2005). To maintain the balance of the farmland which had been occupied by urban development, the local government usually reclaimed the coastal wetland (Tian et al., 2016).

Thirdly, socioeconomic factors apparently had great impacts on the coastal land use land cover changes revealed by canonical correlation analysis (CCA). Furthermore, the partial least square regression analysis demonstrated that the natural and semi-natural land use type, such as fresh water, was mostly negatively driven by some of the socioeconomic factors (Table 2 and Table A.2), which could result in the fluctuation in the areas of natural and semi-natural land use change such as the freshwater surfaces and tidal flat (Fig. 5). While the urban land use type, for example, the public facilities, was positively driven by most of the socioeconomic factors. CCA results displayed that the residential land and public facilities were influenced by foreign investment and real estate, this was possibly due to the high level of association (e.g., similar to collinearity between explanatory variables in a regression analysis) between foreign investment and real estate (Jiang et al., 1998; Sirmans and Worzala, 2003; Wei et al., 2006). Specifically, the magnitude of the positive correlation of foreign investment outweighed that of real estate, suggesting the more important role of foreign investment in urban land growth reflected through the two land-use indicators. Foreign investment zones made Chinese cities, especially those in coastal regions like Shanghai, the most globalized areas absorbing resources from oversee companies to boost its economy and attract labor, hence resulting in the expansion of urban land use such as residential areas to host the in-flow of the population (Wei and Ye, 2014; Wei, 2012). In other words, it implied that the land use land cover changes in the coastal zone were influenced by the combinations of policies and socioeconomic factors in Shanghai, which was similar to the finding of driving factors for the coastal aquaculture expansion in Southeast Asia (Akber et al., 2020).

4.3. Implications and future directions for coastal zone management

This study examined the coastal land use land cover changes and the potential driving factors for each land use type in the past three decades. We revealed the dramatic changes and high dynamics of land use land cover in different time periods and identified dominant socioeconomic factors for specific land use types. These findings can provide several implications for coastal zone planning and management.

First, the fast transformations between land use land cover types, high land use dynamics (Fig. A.2), and the reclamations along the entire coastal line in different time periods imply that there was no comprehensive planning for the coastal zone in the past few decades in Shanghai. On the one hand, the quick-shifting of land use land cover types every five years showed that the land use strategies were considered unstable and could lead to insufficient utilization of land resources. Most of the infrastructures, such as the traffic road, public facilities, and even the industrial and residential areas, did not reach the planned life cycles and were forced to be replaced with or transferred to other land use types, which could result in a waste of land resources and investment. On the other hand, a large amount of natural and semi-natural land had been transformed into artificial land, and coastal wetlands had been reclaimed. Although there were a lot of freshwater surfaces, tidal flats, and farmlands generated, they were the young natural and semi-natural land use land cover types and had been in their earlier succession stage of ecosystems, which cannot function as stable ecosystems can do. More time and conservation efforts are needed to restore these ecosystems. Therefore, comprehensive utilization and protection planning of the coastal zone in Shanghai is urgently needed.

Second, the urbanization degree in the coastal zone in Shanghai had reached a high level and should be controlled. The land urbanization degree reached 41.2% in 2015 and the compound annual growth rate was 4.32% between 1989 and 2015, nearly approaching those of the entire Shanghai, which were 44.1% in 2015 and 4.06% during 1985–2015, respectively (Wu et al., 2023). Our results showed that the proportion of each urban land type exhibited an increasing trend (Fig. 5), and no sign showed that the increase will slow down. A previous study showed that coastal urbanization had caused increased fragmentation and isolation of natural and semi-natural landscapes, and aggregation of artificial landscapes (Li et al., 2009). The latest Shanghai Master Planning (2017–2035) also showed that Shanghai would adopt the bottom-line control policy, which was to strictly abide by the four development baselines, i.e., construction land boundary, population size ceiling, ecological environment boundary, and city safety requirement, to keep a "negative growth" of the overall planned construction land. To fulfill this goal, one of the best approaches was to develop ecological infrastructures, such as green and blue landscapes (Wu et al., 2023). Our driving factor analysis could provide practical ways via regulating the main drivers and the associated investment to well control the growth of target land use types.

Third, the ecosystem services and tradeoff should be conducted in the next step to evaluate the ecological and environmental consequences associated with coastal land use land cover changes and support the decision-making in coastal management in Shanghai. Many studies demonstrated that coastal land use land cover changes have already had impacts on ecosystem services of coastal wetlands (Aitali et al., 2022; Liu et al., 2021; Tiando et al., 2021; Xin et al., 2023), such as the coastal habitat loss and fragmentation (Liu et al., 2022; Xie et al., 2018), habitat declines and the associated ecological risks (Zhai et al., 2020), land use land cover changes in China coastal areas have led to the reduction of ecosystem carbon storage (Zhu et al., 2022), soil carbon and nitrogen losses caused by the conversion of coastal wetland global (Tan et al., 2022), and the warming land surface temperature with marshland conversion to artificial land cover in China (Shen et al., 2020). All these studies are currently hot topics and urgently needed to be addressed to support sustainable development and management of coastal and marine areas. Shanghai, as a coastal global megacity, with a drastic coastal land use land cover change in the past decades, however, still lacks such studies which should be initiated in the near future.

5. Conclusions

This study found that the total land area in the coastal zone of mainland Shanghai increased linearly with time from 1989 to 2015 at an annual rate of 7.6%, primarily as a result of land reclamation. Dramatic conversion between different land use land cover types occurred during the period. The coastal urban land use types increased substantially and the total urbanized land proportion reached 42.1% in 2015. The coastal urbanization was at the cost of natural and semi-natural land. Nearly 64.4% of the agricultural land, 24.4% of ocean area, 84.9% of the fresh water, and 92.8% of the tidal flat within the coastal zone had been converted to urban land during 1989–2015. The spatiotemporal change pattern of land use land cover in each grid along the north-to-south coastal line exhibited an increasing trend of total land resources and urbanization degree and a declining trend of natural and semi-natural land. These patterns could be well matched spatially and temporally with the large constructions of industrial and economic development and decision-making. The coastal land use land cover changes were significantly driven by most of the socioeconomic factors based on the quantitative relationship of canonical correlation analysis established between socioeconomic driving factors and the area of each land use land cover type. The partial least square regression model showed that the majority of socioeconomic factors positively contributed to public facilities increase, and were negatively associated with the area of fresh water. These findings can provide insights for decision-making in the future for coastal land use land cover planning and management in Shanghai.

Appendix

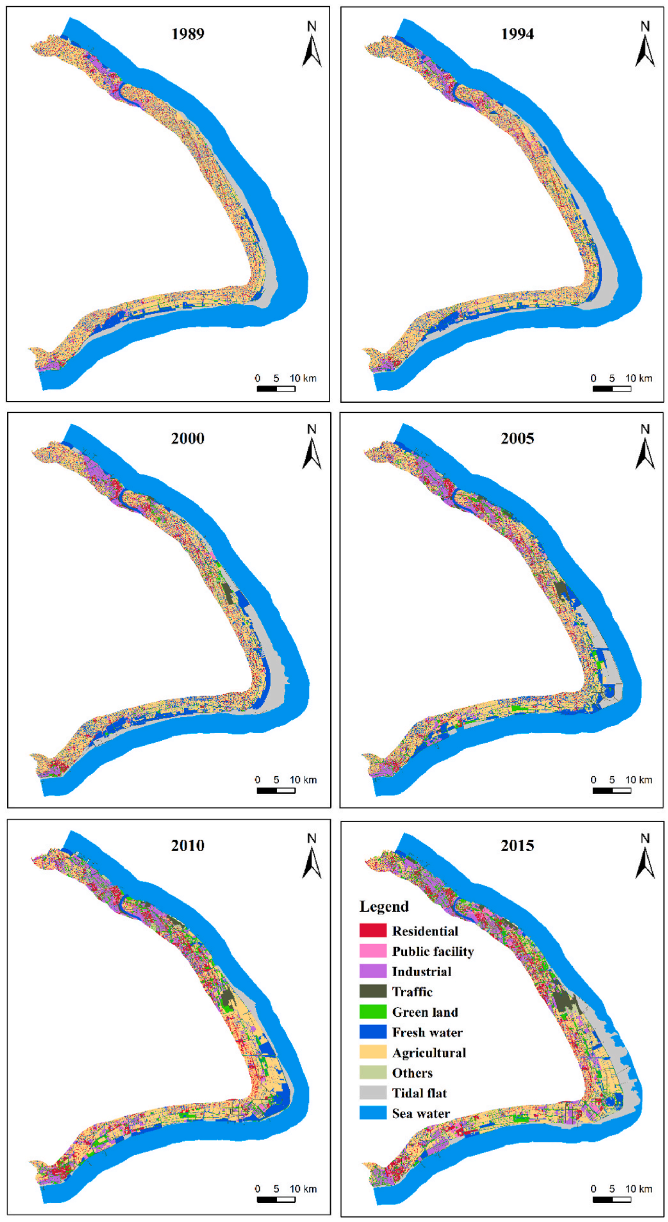

Fig. A.1. The maps of land use land cover in the mainland coastal zone of Shanghai from 1989 to 2015.

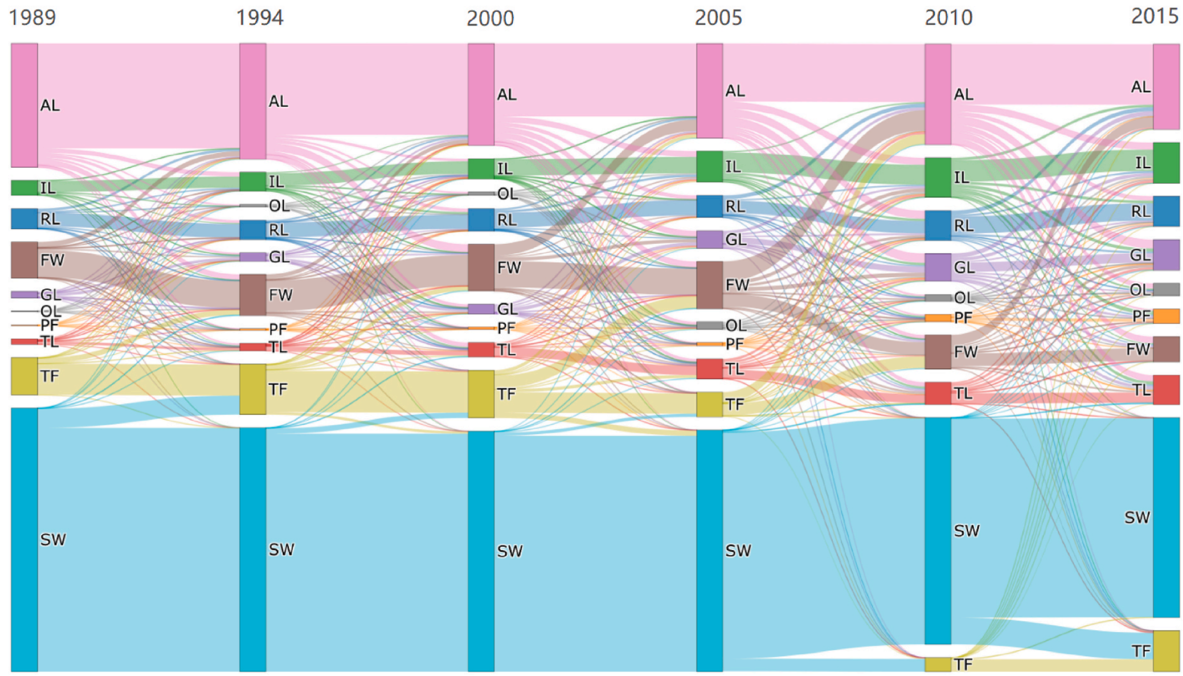

Fig. A.2. The transformation between land use/cover types in each period from 1989 to 2015 in Shanghai coastal zone. RL: Residential land; PF: Public facility; IL: Industrial land; TL: Traffic land; GL: Green land; FW: Fresh water; AL: Agricultural land; OL: Other land (others); TF: Tidal flat; SW: Sea water.

Table A.1
Linear regression analysis between socioeconomic factors and different land use land cover types.

Land use land cover types	Equation	R^2	P value
Residential land	$y = -95.6 + 0.802*X_1$	0.12	0.573
	$y = -22.9 + 406*X_2$	0.34	0.302
	$y = 29.5 + 0.0118*X_3$	0.04	0.732
	$y = -67.1 + 0.0034*X_4$	0.13	0.559
	$y = 35 + 0.0064*X_5$	0.11	0.589
	$y = -183 + 9.06*X_6$	0.71	0.072
	$y = -181 + 0.123*X_7$	0.57	0.138
	$y = 93.5 + 0.0367*X_8$	0.02	0.808
	$y = 77.7 + 0.813*X_9$	0.03	0.766
	$y = -111 + 0.316*X_{10}$	0.52	0.168
Industrial land	$y = -18.6 + 1.39*X_1$	0.21	0.432
	$y = 438\text{-}142*X_2$	0.03	0.797
	$y = 463\text{-}0.0090*X_3$	0.02	0.839
	$y = 308 + 0.0012*X_4$	0.01	0.872
	$y = 393\text{-}0.0007*X_5$	<0.01	0.966
	$y = 36.2 + 9.82*X_6$	0.51	0.173
	$y = 173 + 0.0807*X_7$	0.15	0.515
	$y = 442\text{-}0.0513*X_8$	0.03	0.789
	$y = 455\text{-}1.02*X_9$	0.03	0.770
	$y = 261 + 0.155*X_{10}$	0.08	0.650
Traffic land	$y = 174 + 0.583*X_1$	0.12	0.566
	$y = 324 + 48.4*X_2$	<0.01	0.876
	$y = 163 + 0.0198*X_3$	0.25	0.393
	$y = 175 + 0.0028*X_4$	0.17	0.496
	$y = 262 + 0.0051*X_5$	0.14	0.543
	$y = 444\text{-}2.88*X_6$	0.14	0.533
	$y = 319 + 0.0092*X_7$	<0.01	0.899
	$y = 227 + 0.0991*X_8$	0.33	0.312
	$y = 224 + 1.65*X_9$	0.27	0.364
	$y = 331 + 0.015*X_{10}$	<0.01	0.939
Public facility	$y = 361\text{-}0.543*X_1$	0.08	0.653
	$y = 266\text{-}156*X_2$	0.07	0.663
	$y = -201 + 0.0446*X_3$	0.92	0.010
	$y = -227 + 0.0073*X_4$	0.80	0.040
	$y = -43.8 + 0.0157*X_5$	0.92	0.010

(continued on next page)

Table A.1 (*continued*)

Land use land cover types	Equation	R^2	P value
	$y = 218\text{-}0.377*X_6$	<0.01	0.947
	$y = -14.3 + 0.0844*X_7$	0.39	0.263
	$y = -17.9 + 0.191*X_8$	0.88	0.018
	$y = -50.6 + 3.54*X_9$	0.92	0.009
	$y = -12.2 + 0.277*X_{10}$	0.57	0.141
Green land	$y = 45.1 + 1.09*X_1$	0.17	0.491
	$y = 377\text{-}44.2*X_2$	<0.01	0.928
	$y = 216 + 0.0159*X_3$	0.06	0.680
	$y = 52.5 + 0.0052*X_4$	0.23	0.419
	$y = 229 + 0.0083*X_5$	0.14	0.531
	$y = -8.37 + 10.4*X_6$	0.75	0.059
	$y = -0.21 + 0.139*X_7$	0.58	0.134
	$y = 298 + 0.053*X_8$	0.04	0.754
	$y = 289 + 0.983*X_9$	0.04	0.749
	$y = 91.1 + 0.343*X_{10}$	0.49	0.191
Fresh water	$y = -127\text{-}0.173*X_1$	<0.01	0.961
	$y = -233 + 144*X_2$	<0.01	0.890
	$y = 837\text{-}0.112*X_3$	0.71	0.074
	$y = 1080\text{-}0.0211*X_4$	0.83	0.031
	$y = 498\text{-}0.0428*X_5$	0.84	0.029
	$y = 265\text{-}12.6*X_6$	0.24	0.403
	$y = 739\text{-}0.354*X_7$	0.83	0.030
	$y = 357\text{-}0.458*X_8$	0.63	0.111
	$y = 441\text{-}8.58*X_9$	0.67	0.092
	$y = 623\text{-}1.02*X_{10}$	0.95	0.004
Agricultural land	$y = -860 + 1.12*X_1$	0.04	0.746
	$y = -653 + 295*X_2$	0.03	0.774
	$y = -435\text{-}0.0114*X_3$	<0.01	0.890
	$y = -692 + 0.0026*X_4$	0.01	0.856
	$y = -589 + 0.0032*X_5$	<0.01	0.911
	$y = -1330 + 22.5*X_6$	0.78	0.046
	$y = -1090 = 0.215*X_7$	0.31	0.325
	$y = -426\text{-}0.0955*X_8$	0.03	0.789
	$y = -438\text{-}1.39*X_9$	0.02	0.831
	$y = -958 + 0.538*X_{10}$	0.27	0.370
Other land	$y = 220\text{-}0.166*X_1$	<0.01	0.881
	$y = 293–308*X_2$	0.34	0.298
	$y = -11.8 + 0.0203*X_3$	0.23	0.408
	$y = 6.92 + 0.0028*X_4$	0.15	0.526
	$y = 85.7 + 0.0055*X_5$	0.14	0.536
	$y = 340\text{-}4.76*X_6$	0.35	0.298
	$y = 206\text{-}0.013*X_7$	0.01	0.865
	$y = 57.5 + 0.0987*X_8$	0.29	0.347
	$y = 53.3 + 1.66*X_9$	0.25	0.392
	$y = 189\text{-}0.0213*X_{10}$	<0.01	0.918
Tidal flat	$y = 3200\text{-}10.9*X_1$	0.66	0.094
	$y = 653–1510*X_2$	0.15	0.525
	$y = -1020 + 0.119*X_3$	0.14	0.534
	$y = -431 + 0.0083*X_4$	0.02	0.810
	$y = -481 + 0.0343*X_5$	0.09	0.614
	$y = 1700\text{-}46.7*X_6$	0.58	0.133
	$y = 716\text{-}0.254*X_7$	0.08	0.654
	$y = -561 + 0.533*X_8$	0.15	0.520
	$y = -690 + 10.4*X_9$	0.17	0.486
	$y = 221\text{-}0.206*X_{10}$	<0.01	0.895

Note: X_1: the total length of road, X_2: total length of harbor, X_3: annual Passenger departure, X_4: freight traffic volume, X_5: gross output value of industry, X_6: year-end resident population, X_7: fixed-asset investment, X_8: real estate investment, X_9: foreign direct investment, X_{10}: urban infrastructure investment.

Table A.2
The canonical correlation analysis of the socioeconomic factors and different land use land cover types.

Factors	Canonical variable	Canonical correlation coefficient	P value	Canonical variable expressions
X_5, X_9 & $Y_{residential\ land}$, $Y_{agricultural\ land}$	1	0.9999	0.0257	$u1 = 4.7288*X_5+4.8592*X_9$ $v1 = 0.3469*Y_{residential\ land}-1.2547*Y_{agricultural\ land}$
	2	0.4576	0.5424	
X_1, X_8 & $Y_{residential\ land}$, $Y_{public\ facility}$	1	0.9999	0.0246	$u1 = -0.3607*X_1+0.9336*X_8$ $v1 = -0.2193*Y_{residential\ land}-1.0277*Y_{public\ facility}$
	2	0.3733	0.6267	
X_1, X_9 & $Y_{residential\ land}$, $Y_{public\ facility}$	1	0.9999	0.0283	$u1 = 0.2985*X_1+0.9416*X_9$ $v1 = -0.1648*Y_{residential\ land}+1.0252*Y_{public\ facility}$
	2	0.3905	0.6095	
X_4, X_5 & $Y_{residential\ land}$ & $Y_{public\ facility}$	1	0.9998	0.0349	$u1 = -2.4768*X_5+1.5377*X_4$ $v1 = -0.0411*Y_{residential\ land}-0.9897*Y_{public\ facility}$
	2	0.2644	0.7356	
X_5, X_7 & $Y_{residential\ land}$, $Y_{public\ facility}$	1	0.9992	0.0395	$u1 = -1.5170*X_5+0.8462*X_7$ $v1 = 0.3784*Y_{residential\ land}-1.0172*Y_{public\ facility}$
	2	0.8696	0.1304	
X_8, X_9 & $Y_{residential\ land}$ & $Y_{public\ facility}$	1	0.9997	0.0444	$u1 = 4.2984*X_8-5.2415*X_9$ $v1 = -0.0928*Y_{residential\ land}-0.9745*Y_{public\ facility}$
	2	0.4142	0.5858	
X_4, X_9 & $Y_{green\ land}$, $Y_{public\ facility}$	1	0.9960	0.0545	$u1 = -2.9665*X_4+3.2999*X_9$ $v1 = -0.8691*Y_{green\ land}+0.6649*Y_{public\ facility}$
	2	0.9514	0.0486	$u2 = 1.5712*X_4-0.6161*X_9$ $v2 = 0.5242*Y_{green\ land}+0.7668*Y_{public\ facility}$
X_3, X_9 & $Y_{green\ land}$ & $Y_{public\ facility}$	1	0.9920	0.0696	$u1 = -17.0198*X_3+16.7719*X_9$ $v1 = -0.9962*Y_{green\ land}-0.0211*Y_{public\ facility}$
	2	0.9598	0.0402	$u2 = -3.8365*X_3+ 4.8057*X_9$ $v2 = -0.1941*Y_{green\ land}+1.0147*Y_{public\ facility}$
X_4, X_5& $Y_{green\ land}$, $Y_{public\ facility}$	1	0.9998	0.0305	$u1 = -1.4059*X_4+2.3532*X_5$ $v1 = 0.0515*Y_{green\ land}+0.9899*Y_{public\ facility}$
	2	0.6801	0.3199	
X_3, X_9 & $Y_{industrial\ land}$, $Y_{fresh\ water}$	1	0.9999	0.0160	$u1 = 16.8068*X_3-16.5108*X_9$ $v1 = 0.7660*Y_{industrial\ land}-0.4994*Y_{fresh\ water}$
	2	0.8850	0.1150	
X_1, X_{10} & $Y_{public\ facility}$, $Y_{traffic\ land}$	1	1.0000	0.0142	$u1 = -0.6738*X_1+0.9097*X_{10}$ $v1 = 1.0341*Y_{public\ facility}-0.5159*Y_{traffic\ land}$
	2	0.2985	0.7015	
X_6, X_{10} & $Y_{public\ facility}$, $Y_{traffic\ land}$	1	1.0000	0.0123	$u1 = -0.8637*X_6+1.2742*X_{10}$ $v1 = 0.9719Y_{public\ facility}+0.0800*Y_{traffic\ land}$
	2	0.3782	0.6218	
X_3, X_4 & $Y_{public\ facility}$, $Y_{traffic\ land}$	1	0.9997	0.0479	$u1 = -1.7796*X_3+0.8257*X_4$ $v1 = -0.8797*Y_{public\ facility}-0.2735*Y_{traffic\ land}$
	2	0.2377	0.7623	
X_3, X_8 & $Y_{public\ facility}$, $Y_{traffic\ land}$	1	0.9986	0.0344	$u1 = -5.7537*X_3+6.5833*X_8$ $v1 = 0.4334*Y_{public\ facility}+0.7752*Y_{traffic\ land}$
	2	0.9458	0.0542	$u2 = 9.4149*X_3-8.8547*X_8$ $v2 = 0.9601Y_{public\ facility}-0.7133*Y_{traffic\ land}$
X_4, X_9 & $Y_{public\ facility}$, $Y_{traffic\ land}$	1	1.0000	0.0029	$u1 = 0.5202*X_4-1.4845*X_9$ $v1 = -0.8683*Y_{public\ facility}-0.2933*Y_{traffic\ land}$
	2	0.2746	0.7254	
X_5, X_9 & $Y_{public\ facility}$, $Y_{traffic\ land}$	1	1.0000	0.0124	$u1 = 1.1260*X_5-2.0747*X_9$ $v1 = -0.7783*Y_{public\ facility}-0.4292*Y_{traffic\ land}$
	2	0.7667	0.2333	
X_7, X_{10} & $Y_{agricultural\ land}$, $Y_{traffic\ land}$	1	0.9999	0.0335	$u1 = -2.6519*X_7+1.7645*X_{10}$ $v1 = -1.4803*Y_{agricultural\ land}-1.2243*Y_{traffic\ land}$
	2	0.1000	0.9000	
X_1, X_3 & $Y_{agricultural\ land}$, $Y_{traffic\ land}$	1	1.0000	0.0173	$u1 = 0.7717*X_1+0.6525*X_3$

(continued on next page)

Table A.2 (*continued*)

Factors	Canonical variable	Canonical correlation coefficient	P value	Canonical variable expressions
				$v1 = 1.2006*Y_{agricultural\ land}+1.4849*Y_{traffic\ land}$
	2	0.1940	0.8060	
X_1, X_5 & $Y_{agricultural\ land}$, $Y_{traffic\ land}$	1	0.9999	0.0237	$u1 = 0.7791*X_1+0.6418*X_5$ $v1 = 1.2859*Y_{agricultural\ land}+1.4617*Y_{traffic\ land}$
	2	0.0739	0.9261	
X_1, X_8 & $Y_{agricultural\ land}$, $Y_{traffic\ land}$	1	1.0000	0.0183	$u1 = 0.7475*X_1+0.6625*X_8$ $v1 = 1.1461*Y_{agricultural\ land}+1.4910*Y_{traffic\ land}$
	2	0.2584	0.7416	
X_1, X_9 & $Y_{agricultural\ land}$, $Y_{traffic\ land}$	1	0.9999	0.0205	$u1 = 0.7822*X_1+0.6577*X_9$ $v1 = 1.1740*Y_{agricultural\ land}+1.4885*Y_{traffic\ land}$
	2	0.2265	0.7735	
X_3, X_8 & $Y_{agricultural\ land}$, $Y_{traffic\ land}$	1	0.9999	0.0235	$u1 = 9.5573*X_3-10.0177*X_8$ $v1 = 0.2534*Y_{agricultural\ land}-0.7974*Y_{traffic\ land}$
	2	0.5523	0.4477	
X_4, X_8 & $Y_{tidal\ flat}$, $Y_{traffic\ land}$	1	1.0000	0.0071	$u1 = 2.6626*X_4-3.1496*X_8$ $v1 = -0.7065*Y_{tidal\ flat}-0.5832*Y_{traffic\ land}$
	2	0.2458	0.7542	
X_4, X_{10} & $Y_{other\ land}$, $Y_{green\ land}$	1	1.0000	0.0137	$u1 = -2.1436*X_4+2.1753*X_{10}$ $v1 = 0.2923*Y_{green\ land}-0.8909*Y_{other\ land}$
	2	0.6775	0.3225	
X_8, X_{10} & $Y_{other\ land}$, $Y_{green\ land}$	1	0.9997	0.0375	$u1 = 1.3324*X_8-1.4530*X_{10}$ $v1 = -0.5967*Y_{green\ land}+0.67587*Y_{other\ land}$
	2	0.6008	0.3992	
X_1, X_5 & $Y_{other\ land}$, $Y_{residential\ land}$	1	0.9997	0.0450	$u1 = -0.36261*X_1-0.9388*X_5$ $v1 = -1.3637*Y_{residential\ land}-1.2962\ Y_{other\ land}$
	2	0.2278	0.7722	
X_8, X_{10} & $Y_{other\ land}$, $Y_{industrial\ land}$	1	1.0000	0.0149	$u1 = -1.4741*X_8+1.2850*X_{10}$ $v1 = 0.4807*Y_{industrial\ land}-0.8068*Y_{other\ land}$
	2	0.2123	0.7877	
X_4, X_{10} & $Y_{other\ land}$, $Y_{industrial\ land}$	1	0.9997	0.0477	$u1 = -2.2043*X_4+2.0897*X_{10}$ $v1 = 0.2174*Y_{industrial\ land}-0.9436*Y_{other\ land}$
	2	0.2536	0.7464	
X_4, X_8 & $Y_{other\ land}$, $Y_{industrial\ land}$	1	0.9998	0.0317	$u1 = -3.0625*X_4+3.3309*X_8$ $v1 = -0.7842*Y_{industrial\ land}+0.5125*Y_{other\ land}$
	2	0.3999	0.6001	
X_6, X_7 & $Y_{fresh\ water}$, $Y_{agricultural\ land}$	1	0.9998	0.0186	$u1 = 1.2010*X_6-1.4624*X_7$ $v1 = 1.0941*Y_{fresh\ water}+0.7478*Y_{agricultural\ land}$
	2	0.8871	0.1129	
X_1, X_9 & $Y_{fresh\ water}$, $Y_{agricultural\ land}$	1	1.0000	0.0137	$u1 = 0.0550*X_1-0.9961*X_9$ $v1 = 1.1159*Y_{fresh\ water}+0.6596*Y_{agricultural\ land}$
	2	0.1894	0.8106	
X_3, X_4 & $Y_{fresh\ water}$, $Y_{agricultural\ land}$	1	1.0000	0.0030	$u1 = -1.4920*X_3+0.5158*X_4$ $v1 = 1.1077*Y_{fresh\ water}+0.6991*Y_{agricultural\ land}$
	2	0.7981	0.2019	
X_3, X_5 & $Y_{fresh\ water}$, $Y_{agricultural\ land}$	1	0.9989	0.0179	$u1 = 1.0582*X_3-2.030711*X_5$ $v1 = 1.0966*Y_{fresh\ water}+0.2736*Y_{agricultural\ land}$
	2	0.9809	0.0191	
X_3, X_6 & $Y_{fresh\ water}$, $Y_{agricultural\ land}$	1	0.9991	0.0383	$u1 = -0.9962*X_3+0.1394*X_6$ $v1 = 1.1026*Y_{fresh\ water}+0.7190*Y_{agricultural\ land}$
	2	0.8879	0.1121	
X_3, X_7 & $Y_{fresh\ water}$, $Y_{agricultural\ land}$	1	0.9988	0.0468	$u1 = -1.1150*X_3+0.1732*X_7$ $v1 = 1.1063*Y_{fresh\ water}+0.7049*Y_{agricultural\ land}$
	2	0.8795	0.1205	
X_3, X_8 & $Y_{fresh\ water}$, $Y_{agricultural\ land}$	1	0.9994	0.0312	$u1 = -2.6628*X_3+1.6814*X_8$ $v1 = 1.1262*Y_{fresh\ water}+0.4700*Y_{agricultural\ land}$
	2	0.8949	0.1051	
X_4, X_9 & $Y_{fresh\ water}$, $Y_{agricultural\ land}$	1	0.9997	0.0308	$u1 = 0.2723*X_4-1.2566*X_9$ $v1 = 1.1052*Y_{fresh\ water}+0.7093*Y_{agricultural\ land}$
	2	0.8101	0.1899	

(*continued on next page*)

Table A.2 (*continued*)

Factors	Canonical variable	Canonical correlation coefficient	P value	Canonical variable expressions
X_4, X_5 & $Y_{fresh\ water}$, $Y_{agricultural\ land}$	1	0.9997	0.0437	$u1 = 0.3027*X_4-1.2966*X_5$ $v1 = 1.1259*Y_{fresh\ water}+0.4642*Y_{agricultural\ land}$
	2	0.2579	0.7421	
X_4, X_8 & $Y_{fresh\ water}$, $Y_{agricultural\ land}$	1	0.9993	0.0310	$u1 = -0.8829*X_4+1.8075*X_8$ $v1 = -1.0327*Y_{fresh\ water}-0.8788*Y_{agricultural\ land}$
	2	0.9142	0.0858	$u1 = 3.2356*X_4-2.8251*X_8$ $v1 = -0.4528*Y_{fresh\ water}+0.7066*Y_{agricultural\ land}$
X_5, X_9 & $Y_{fresh\ water}$, $Y_{agricultural\ land}$	1	0.9986	0.0193	$u1 = -0.4310*X_5-0.5742*X_9$ $v1 = 1.1264*Y_{fresh\ water}+0.5672*Y_{agricultural\ land}$
	2	0.9824	0.0176	$u1 = -4.8418*X_5+4.8269*X_9$ $v1 = 0.0526*Y_{fresh\ water}-0.97461*Y_{agricultural\ land}$
X_5, X_6 & $Y_{fresh\ water}$, $Y_{agricultural\ land}$	1	0.9990	0.0412	$u1 = -1.0097*X_5+0.0736*X_6$ $v1 = 1.1276*Y_{fresh\ water}+0.5159*Y_{agricultural\ land}$
	2	0.8879	0.1121	
X_6, X_8 & $Y_{fresh\ water}$, $Y_{agricultural\ land}$	1	0.9990	0.0417	$u1 = 0.2214*X_6-0.9726*X_8$ $v1 = 1.0528*Y_{fresh\ water}+0.8449*Y_{agricultural\ land}$
	2	0.8823	0.1177	
X_6, X_9 & $Y_{fresh\ water}$, $Y_{agricultural\ land}$	1	0.9999	0.0104	$u1 = 0.1153*X_6-0.9928*X_9$ $v1 = 1.0962*Y_{fresh\ water}+0.7411*Y_{agricultural\ land}$
	2	0.8873	0.1127	
X_7, X_9 & $Y_{fresh\ water}$, $Y_{agricultural\ land}$	1	0.9999	0.0136	$u1 = 0.1527*X_7-1.0967*X_9$ $v1 = 1.0969*Y_{fresh\ water}+0.7389*Y_{agricultural\ land}$
	2	0.8854	0.1146	
X_8, X_9 & $Y_{fresh\ water}$, $Y_{agricultural\ land}$	1	0.9998	0.0358	$u1 = 0.8238*X_8-1.8201*X_9$ $v1 = 1.1214*Y_{fresh\ water}+0.6237*Y_{agricultural\ land}$
	2	0.4900	0.5100	

Note: X_1: the total length of road, X_2: total length of harbor, X_3: annual passenger departure, X_4: freight traffic volume, X_5: gross output value of industry, X_6: year-end resident population, X_7: fixed-asset investment, X_8: real estate investment, X_9: foreign direct investment, X_{10}: urban infrastructure investment.

Declaration of competing interest

The authors declare that they have no known competing financial interests or personal relationships that could have appeared to influence the work reported in this paper.

Data availability

Data will be made available on request.

Acknowledgments

We are grateful to three anonymous reviewers for their valuable and constructive comments and suggestions. We are also grateful to Meng Wang, Linke Ouyang, Yuhan Liu, Jing Gao, Shengzi Chen, Yu Chen, Yue Huang, and Shuya Fan for their assistance with the digitization of aerial photos. This study was partly supported by the Natural Science Foundation of China (Grant No. 32001162, Grant No. 31971485), National Key R&D Program of China (Grant No. 2017YFC0505801), and China Postdoctoral Science Foundation 2021M702131.

References

Aitali, R., Snoussi, M., Kolker, A.S., Oujidi, B., Mhammdi, N., 2022. Effects of land use/land cover changes on carbon storage in north African coastal wetlands. J. Mar. Sci. Eng. 10, 364.

Akber, M.A., Aziz, A.A., Lovelock, C., 2020. Major drivers of coastal aquaculture expansion in Southeast Asia. Ocean Coast Manag. 198, 105364.

An, S., Li, H., Guan, B., Zhou, C., Wang, Z., Deng, Z., Zhi, Y., Liu, Y., Xu, C., Fang, S., Jiang, J., Li, H., 2007. China's natural wetlands: past problems, current status, and future challenges. AMBIO A J. Hum. Environ. 36, 335–342, 338.

Arkema, K.K., Verutes, G.M., Wood, S.A., Clarke-Samuels, C., Rosado, S., Canto, M., Rosenthal, A., Ruckelshaus, M., Guannel, G., Toft, J., Faries, J., Silver, J.M., Griffin, R., Guerry, A.D., 2015. Embedding ecosystem services in coastal planning leads to better outcomes for people and nature. Proc. Natl. Acad. Sci. USA 112, 7390–7395.

Barbier, E.B., Hacker, S.D., Kennedy, C., Koch, E.W., Stier, A.C., Silliman, B.R., 2011. The value of estuarine and coastal ecosystem services. Ecol. Monogr. 81, 169–193.

Bracchetti, L., Carotenuto, L., Catorci, A., 2012. Land-cover changes in a remote area of central Apennines (Italy) and management directions. Landsc. Urban Plann. 104, 157–170.

Brandt, J., Primdahl, J., Reenberg, A., 1999. Rural land-use and dynamic forces – analysis of 'driving forces' in space and time. In: Krönert, R., Baudry, J., Bowler, I., Reenberg, A. (Eds.), Land-use Changes and Their Environmental Impact in Rural Areas in Europe. UNESCO Paris, pp. 82–102.

Cao, W., Wong, M.H., 2007. Current status of coastal zone issues and management in China: a review. Environ. Int. 33, 985–992.

Cazenave, A., Cozannet, G.L., 2014. Sea level rise and its coastal impacts. Cazenave and Le Cozannet 2, 15–34.

Chen, Z., Li, B., Zhong, Y., Chen, J., 2004. Local competitive effects of introduced Spartina alterniflora on Scirpus mariqueter at Dongtan of Chongming Island, the Yangtze River estuary and their potential ecological consequences. Hydrobiologia 528, 99–106.

Chmura, G.L., Anisfeld, S.C., Cahoon, D.R., Lynch, J.C., 2003. Global carbon sequestration in tidal, saline wetland soils. Global Biogeochem. Cycles 17.

Chuai, X.W., Wen, J.Q., Zhuang, D.C., Guo, X.M., Yuan, Y., Lu, Y., Zhang, M., Li, J.S., 2019. Intersection of physical and Anthropogenic effects on land-use/land-cover changes in coastal China of Jiangsu province. Sustainability-Basel 11.

Crain, C.M., Halpern, B.S., Beck, M.W., Kappel, C.V., 2009. Understanding and managing human threats to the coastal marine environment. The Year in Ecology and Conservation Biology 1162, 39–62.

de Andrés, M., Barragán Muñoz, J.M., García Onetti, J., Chavarria Zuniga, L.D., 2023. Mapping services for an ecosystem based management along the Andalusian coastal zone (Spain). Ocean Coast Manag. 231, 106402.

Eddy, I.S., Gergel, S., 2015. Why landscape ecologists should contribute to life cycle sustainability approaches. Landsc. Ecol. 30, 215–228.
Ekumah, B., Armah, F.A., Afrifa, E.K.A., Aheto, D.W., Odoi, J.O., Afitiri, A.R., 2020. Assessing land use and land cover change in coastal urban wetlands of international importance in Ghana using Intensity Analysis. Wetl. Ecol. Manag. 28, 271–284.
Grimm, L.G., Yarnold, P.R., 2000. Reading and Understanding MORE Multivariate Statistics. American psychological association.
Guan, D., Li, H., Inohae, T., Su, W., Nagaie, T., Hokao, K., 2011. Modeling urban land use change by the integration of cellular automaton and Markov model. Ecol. Model. 222, 3761–3772.
Härdle, W.K., Simar, L., 2019. Canonical Correlation Analysis.
Huang, Z., He, C., Wei, Y.H.D., 2016. A comparative study of land efficiency of electronics firms located within and outside development zones in Shanghai. Habitat Int. 56, 63–73.
Irwin, E.G., Bockstael, N.E., 2007. The evolution of urban sprawl: evidence of spatial heterogeneity and increasing land fragmentation. Proc. Natl. Acad. Sci. USA 104, 20672–20677.
Jiang, D., Chen, J.J., Isaac, D., 1998. The effect of foreign investment on the real estate industry in China. Urban Stud. 35, 2101–2110.
Kankam, S., Osman, A., Inkoom, J.N., Fürst, C., 2022. Implications of spatio-temporal land use/cover changes for ecosystem services supply in the coastal landscapes of southwestern Ghana, west Africa. Land 11, 1408.
Kayhko, N., Fagerholm, N., Asseid, B.S., Mzee, A.J., 2011. Dynamic land use and land cover changes and their effect on forest resources in a coastal village of Matemwe, Zanzibar, Tanzania. Land Use Pol. 28, 26–37.
Li, C., Li, J., Wu, J., 2018. What drives urban growth in China? A multi-scale comparative analysis. Appl. Geogr. 98, 43–51.
Li, J., Li, C., Zhu, F., Song, C., Wu, J., 2013. Spatiotemporal pattern of urbanization in Shanghai, China between 1989 and 2005. Landsc. Ecol. 28, 1545–1565.
Li, R., Li, J., Li, C., Qin, H., Xu, M., Zhang, T., 2009. Spatiotemporal dynamics of coastal landscape pattern of Shanghai during its rapid urbanization. Chinese Journl of Ecology 28, 2353–2359.
Li, X., Sun, L., 1997. Driving Forces of Arable Land Conversion in China International Institute for Applied Systems Analysis (IIASA) (Laxenburg, Austria).
Li, X., Zhang, Y., Bao, Y., Luo, J., Jin, X., Xu, X., Song, X., Yang, G., 2014. Exploring the best hyperspectral features for LAI estimation using partial least squares regression. Rem. Sens. 6, 6221–6241.
Liu, C., Yang, M., Hou, Y., Xue, X., 2021. Ecosystem service multifunctionality assessment and coupling coordination analysis with land use and land cover change in China's coastal zones. Sci. Total Environ. 797, 149033.
Liu, L., Wang, H.-j., Yue, Q., 2020a. China's coastal wetlands: ecological challenges, restoration, and management suggestions. Regional Studies in Marine Science 37, 101337.
Liu, M., Leung, F., Lee, S.-Y., 2022. Interpreting mangrove habitat and coastal land cover change in the greater bay area, southern China, from 1924 to 2020 using historical aerial photos and multiple sources of satellite data. Rem. Sens. 14, 5163.
Liu, Y., Hou, X., Li, X., Song, B., Wang, C., 2020b. Assessing and predicting changes in ecosystem service values based on land use/cover change in the Bohai Rim coastal zone. Ecol. Indicat. 111, 106004.
Lu, L., Qureshi, S., Li, Q., Chen, F., Shu, L., 2022. Monitoring and projecting sustainable transitions in urban land use using remote sensing and scenario-based modelling in a coastal megacity. Ocean Coast Manag. 224, 106201.
Luan, H.L., Ding, P.X., Wang, Z.B., Ge, J.Z., Yang, S.L., 2016. Decadal morphological evolution of the Yangtze Estuary in response to river input changes and estuarine engineering projects. Geomorphology 265, 12–23.
Marraccini, E., Debolini, M., Moulery, M., Abrantes, P., Bouchier, A., Chéry, J.P., Sanz Sanz, E., Sabbatini, T., Napoleone, C., 2015. Common features and different trajectories of land cover changes in six Western Mediterranean urban regions. Appl. Geogr. 62, 347–356.
Martins, J.H., Camanho, A.S., Gaspar, M.B., 2012. A review of the application of driving forces – pressure – State – impact – Response framework to fisheries management. Ocean Coast Manag. 69, 273–281.
McGranahan, G., Balk, D., Anderson, B., 2007. The Rising Tide: Assessing the Risks of Climate Change and Human Settlements in Low Elevation Coastal Zones, 19. Environment & Urbanization, pp. 17–37.
Mitsuda, Y., Ito, S., 2011. A review of spatial-explicit factors determining spatial distribution of land use/land-use change. Landsc. Ecol. Eng. 7, 117–125.
Olaniyi, A.O., Abdullah, A.M., Ramli, M.F., Alias, M.S., 2012. Assessment of drivers of coastal land use change in Malaysia. Ocean Coast Manag. 67, 113–123.
Pan, M., Hu, T., Zhan, J., Hao, Y., Li, X., Zhang, L., 2023. Unveiling spatiotemporal dynamics and factors influencing the provision of urban wetland ecosystem services using high-resolution images. Ecol. Indicat. 151, 110305.
Pontius, R.G., Shusas, E., McEachern, M., 2004. Detecting important categorical land changes while accounting for persistence. Agric. Ecosyst. Environ. 101, 251–268.
Sannigrahi, S., Joshi, P.K., Keesstra, S., Paul, S.K., Sen, S., Roy, P.S., Chakraborti, S., Bhatt, S., 2019. Evaluating landscape capacity to provide spatially explicit valued ecosystem services for sustainable coastal resource management. Ocean Coast Manag. 182, 104918.
SBS, S.B.o.S., 2019. Shanghai Statistical Yearbook China Statistics Press, Beijing.
Seto, K.C., Güneralp, B., Hutyra, L.R., 2012. Global forecasts of urban expansion to 2030 and direct impacts on biodiversity and carbon pools. Proc. Natl. Acad. Sci. USA 109, 16083–16088.
Shen, X., Liu, B., Jiang, M., Lu, X., 2020. Marshland loss warms local land surface temperature in China. Geophys. Res. Lett. 47, e2020GL087648.
Shi, Y., Wang, H., Li, J., 2003. The actuality and trend for the coastal belt's resource of Shanghai (in Chinese with English abstract). Shanghai Geol. 8–16.
Shi, Z.H., Ai, L., Li, X., Huang, X.D., Wu, G.L., Liao, W., 2013. Partial least-squares regression for linking land-cover patterns to soil erosion and sediment yield in watersheds. J. Hydrol. 498, 165–176.
Sirmans, C.F., Worzala, E., 2003. International direct real estate investment: a review of the literature. Urban Stud. 40, 1081–1114.
Su, D., 2003. Current situation and planning of tidal flat development and utilization in Shanghai (in Chinese with English abstract). Shanghai Construction Science & Technology 18–19.
Sun, Z., Sun, W., Tong, C., Zeng, C., Yu, X., Mou, X., 2015. China's coastal wetlands: conservation history, implementation efforts, existing issues and strategies for future improvement. Environ. Int. 79, 25–41.
Tan, L., Ge, Z., Ji, Y., Lai, D.Y.F., Temmerman, S., Li, S., Li, X., Tang, J., 2022. Land use and land cover changes in coastal and inland wetlands cause soil carbon and nitrogen loss. Global Ecol. Biogeogr. 31, 2541–2563.
Temmerman, S., Meire, P., Bouma, T.J., Herman, P.M.J., Ysebaert, T., De Vriend, H.J., 2013. Ecosystem-based coastal defence in the face of global change. Nature 504, 79–83.
Tian, B., Wu, W., Yang, Z., Zhou, Y., 2016. Drivers, trends, and potential impacts of long-term coastal reclamation in China from 1985 to 2010. Estuar. Coast Shelf Sci. 170, 83–90.
Tiando, D.S., Hu, S., Fan, X., Ali, M.R., 2021. Tropical coastal land-use and land cover changes impact on ecosystem service value during rapid urbanization of Benin, west Africa. Int. J. Environ. Res. Publ. Health 18, 7416.
Turner, M.G., 2005. Landscape ecology in North America: past, present, and future. Ecology 86, 1967–1974.
Urban, D.L., Wallin, D.O., 2002. Introduction to Markov Models. In: Gergel, S.E., Turner, M.G. (Eds.), Learning Landscape Ecology. Springer, New York, NY. https://doi.org/10.1007/0-387-21613-8_4.
Valiela, I., Kinney, E., Peacok, E., Smith, S., Culbertson, J., 2009. Global losses of mangroves and salt marshes. In: Duarte, C.M. (Ed.), Global Loss of Coastal Habitats Rates, Causes and Consequences, p. 22.
Wang, P., Wang, J., Zhang, J., Ma, X., Zhou, L., Sun, Y., 2022. Spatial-temporal changes in ecosystem services and social-ecological drivers in a typical coastal tourism city: a case study of Sanya, China. Ecol. Indicat. 145, 109607.
Wang, W., Liu, H., Li, Y., Su, J., 2014. Development and management of land reclamation in China. Ocean Coast Manag. 102, 415–425.
Wei, Y.D., Leung, C.K., Luo, J., 2006. Globalizing Shanghai: foreign investment and urban restructuring. Habitat Int. 30, 231–244.
Wei, Y.D., Ye, X., 2014. Urbanization, urban land expansion and environmental change in China. Stoch. Environ. Res. Risk Assess. 28, 757–765.
Wei, Y.H.D., 2012. Restructuring for growth in urban China: transitional institutions, urban development, and spatial transformation. Habitat Int. 36, 396–405.
Wold, S., Sjöström, M., Eriksson, L., 2001. PLS-regression: a basic tool of chemometrics. Chemometr. Intell. Lab. Syst. 58, 109–130.
Wu, C., Li, C., Ouyang, L., Xiao, H., Wu, J., Zhuang, M., Bi, X., Li, J., Wang, C., Song, C., Qiu, T., Haase, D., Hahs, A., Finka, M., 2023. Spatiotemporal evolution of urbanization and its implications to urban planning of the megacity, Shanghai, China. Landsc. Ecol. 38, 1105–1124.
Wu, F., 2000. The global and local dimensions of place-making: remaking Shanghai as a world city. Urban Stud. 37, 1359–1377.
Wu, W., Yang, Z., Tian, B., Huang, Y., Zhou, Y., Zhang, T., 2018. Impacts of coastal reclamation on wetlands: loss, resilience, and sustainable management. Estuar. Coast Shelf Sci. 210, 153–161.
Xie, Y., Mei, Y., Guangjin, T., Xuerong, X., 2005. Socio-economic driving forces of arable land conversion: a case study of Wuxian City, China. Global Environ. Change Part A 15, 238–252.
Xie, Y., Yu, X., Ng, N.C., Li, K., Fang, L., 2018. Exploring the dynamic correlation of landscape composition and habitat fragmentation with surface water quality in the Shenzhen river and deep bay cross-border watershed, China. Ecol. Indicat. 90, 231–246.
Xin, X., Zhang, T., He, F., Zhang, W., Chen, K., 2023. Assessing and simulating changes in ecosystem service value based on land use/cover change in coastal cities: a case study of Shanghai, China. Ocean Coast Manag. 239, 106591.
Yang, H., Ma, M., Thompson, J.R., Flower, R.J., 2017. Protect coastal wetlands in China to save endangered migratory birds. Proc. Natl. Acad. Sci. USA 114, E5491–E5492.
Yim, J., Kwon, B.-O., Nam, J., Hwang, J.H., Choi, K., Khim, J.S., 2018. Analysis of forty years long changes in coastal land use and land cover of the Yellow Sea: the gains or losses in ecosystem services. Environ. Pollut. 241, 74–84.
Yu, D., Qiao, J., Shi, P., 2018. Spatiotemporal patterns, relationships, and drivers of China's agricultural ecosystem services from 1980 to 2010: a multiscale analysis. Landsc. Ecol. 33, 575–595.
Yu, W., Zhou, W., Qian, Y., Yan, J., 2016. A new approach for land cover classification and change analysis: integrating backdating and an object-based method. Rem. Sens. Environ. 177, 37–47.
Zhai, T., Wang, J., Fang, Y., Qin, Y., Huang, L., Chen, Y., 2020. Assessing ecological risks caused by human activities in rapid urbanization coastal areas: towards an integrated approach to determining key areas of terrestrial-oceanic ecosystems preservation and restoration. Sci. Total Environ. 708, 135153.
Zhang, W., Chang, W.J., Zhu, Z.C., Hui, Z., 2020a. Landscape ecological risk assessment of Chinese coastal cities based on land use change. Appl. Geogr. 117, 102174.
Zhang, Y., Chen, R., Wang, Y., 2020b. Tendency of land reclamation in coastal areas of Shanghai from 1998 to 2015. Land Use Pol. 91, 104370.
Zhou, D., Wang, S., Liang, X., Wang, J., Zhu, X., Ning, Y., 2021. The relationship between the oxidative stress reaction and the microbial community by a combinative method of PA and CCA. Sci. Total Environ. 763, 143042.

Zhu, L., Song, R., Sun, S., Li, Y., Hu, K., 2022. Land use/land cover change and its impact on ecosystem carbon storage in coastal areas of China from 1980 to 2050. Ecol. Indicat. 142, 109178.

Zhu, Y., Geiß, C., So, E., 2021. Image super-resolution with dense-sampling residual channel-spatial attention networks for multi-temporal remote sensing image classification. Int. J. Appl. Earth Obs. Geoinf. 104, 102543.

Ziaul Hoque, M., Islam, I., Ahmed, M., Shamim Hasan, S., Ahmed Prodhan, F., 2022. Spatio-temporal changes of land use land cover and ecosystem service values in coastal Bangladesh. The Egyptian Journal of Remote Sensing and Space Science 25, 173–180.

Zong, S., Hu, Y., Bai, Y., Guo, Z., Wang, J., 2022. Analysis of the distribution characteristics and driving factors of land use conflict potentials in the Bohai Rim coastal zone. Ocean Coast Manag. 226, 106260.